5.0 STRUCTURES

5.1 CONTAINMENT STRUCTURE

5.1.1 DESIGN BASIS

General plans at various elevations and sections through the Containment Structure interior are shown in Figures 1-6 through 1-15 and show the general arrangement of various equipment such as reactor, steam generators, pressurizer and reactor coolant pumps. The support and anchorage details of these components are shown in Figures 5-11 through 5-15. At an Elevation 177'0", a landing platform, to the ladder on the vent stack provides an access route to the top of the Containment Structure. A steel ladder, provided inside the Containment Structure provides an access up to the polar crane. The Containment Structure is a Seismic Category I structure and is designed for all loading combinations described in Section 5A.3.

The Containment Structure completely encloses the Reactor Coolant System (RCS) to minimize release of radioactive material to the environment should a serious failure of the RCS occur. The structure provides adequate biological shielding for both normal operation and accident situations. The Containment Structure is designed for maximum of 0.16%/day leakage by weight of the original content of air at a design pressure of 50 psig and a concrete surface temperature of 276°F.

The principal design basis for the structure is that it be capable of withstanding the internal pressure resulting from a loss-of-coolant accident (LOCA) with no loss of integrity. In this event, the total energy contained in the water of the RCS is assumed to be released into the Containment Structure through a break in the reactor coolant piping. Subsequent pressure behavior is determined by the building volume, engineered safety features, and the combined influence of energy sources and heat sinks.

Energy is available for release into the Containment Structure from the following sources:

RCS Stored Heat
Reactor Stored Heat
Reactor Decay Heat
Metal-Water Reactions

The energy release and the containment pressure transient curves are shown in Section 14.20.

The design of the engineered safety features systems and their operation is discussed more fully in Chapter 6; only their relation to the basis of Containment Structure design is discussed below. The engineered safety features systems are provided to limit the consequences of an accident. Their energy removal capabilities limit the internal pressure so that Containment Structure design limits are not exceeded and the potential for release of fission products is minimized.

The safety injection systems inject borated water into the reactor vessel to remove core decay heat and to minimize metal-water reactions and the associated release of heat and fission products. Flashed primary coolant, RCS sensible heat, and core decay heat transferred to the Containment Structure are removed by the Containment Cooling System which is comprised of two subsystems; the containment spray subsystem and the air recirculation subsystem.

The containment spray subsystem reduces pressure in the containment by condensing the Containment Structure steam and removing heat from the containment atmosphere by recirculation of the spray water through the shutdown cooling heat exchangers.

The air recirculation subsystem reduces pressure and removes heat directly from the Containment Structure atmosphere to the Service Water System with recirculating fans and cooling coils.

5.1.2 DESIGN CRITERIA

5.1.2.1 General Description

The Containment Structure houses the RCS. Its purpose is to contain any accidental release of radioactivity from the RCS. It is designated as a Seismic Category I structure.

The basic design criteria are that the integrity of the liner plate be guaranteed under all loading conditions and the structure shall have a low-strain elastic response such that its behavior will be predictable under all design loadings.

The structure consists of a post-tensioned reinforced concrete cylinder and dome connected to and supported by a massive reinforced concrete foundation slab as shown in Figure 5-1. The entire interior surface of the structure was lined with a 1/4" thick welded American Society for Testing and Materials (ASTM) A36 steel plate to assure a high degree of leak tightness. Numerous mechanical and electrical systems penetrate the Containment Structure wall through welded steel penetrations as shown in Figures 5-2 and 5-3. The penetrations and access openings were designed, fabricated, inspected, and installed in accordance with the American Society of Mechanical Engineers (ASME), Boiler and Pressure Vessel (B&PV) Code, Section III, Class B.

Principal dimensions of the Containment Structure are:

Inside Diameter	130'
Inside Height (including Dome)	181-2/3'
Vertical Wall Thickness	3-3/4'
Dome thickness	3-1/4'
Foundation Slab Thickness	10'
Liner Plate Thickness	1/4"
Internal Free Volume	1,989,000 ft^3

The Containment Structure is shown in Figures 1-6 through 1-16.

In the concept of a post-tensioned Containment Structure, the internal pressure load is balanced by the application of an opposing external force on the structure. Sufficient post-tensioning was used on the cylinder and dome to more than balance the internal pressure so that a margin of external pressure exists beyond that required to resist the LOCA pressure. See Appendix 5E for an evaluation that reduced the original containment minimum design prestress. Nominal, bonded reinforcing steel was also provided to distribute strains due to shrinkage and temperature. Additional bonded reinforcing steel was used at penetrations and discontinuities to resist local moments and shears.

The internal pressure loads on the foundation slab are resisted by both the external bearing pressure due to dead load and the strength of the reinforced concrete slab. Thus, post-tensioning was not required to exert an external pressure for this portion of the structure.

The post-tensioning system consists of:

a. Three groups of 68 dome tendons oriented at 60° to each other for a total of 204 tendons anchored at the vertical face of the dome ring girder.
b. Two hundred four vertical tendons anchored at the top surface of the ring girder and at the bottom of the base slab.
c. Six groups of 78 hoop tendons, each enclosing 120° of arc, for a total of 468 tendons anchored at the 6 vertical buttresses.

Each tendon consists of approximately 90 1/4" diameter wires with button-headed BBRV-type anchorages, furnished by the Prescon Corporation. The tendons are housed in spiral wrapped, corrugated, thin-wall, carbon steel sheathing. After fabrication, the tendon was shop dipped in a petrolatum corrosion protection material, bagged and shipped. After installation, the tendon sheathing was filled with a corrosion preventive grease (Viconorust 2090P). The ends of all tendons were covered with pressure-tight, grease-filled caps for corrosion protection. All the vertical tendons for each Unit received new corrosion preventive grease between 1997 and the end of 2002. Some original vertical tendons for each Unit were restressed or replaced with a new tendon between 2001 and 2002. See Appendix 5E for details.

American Society for Testing and Materials A615, Grade 60 reinforcing steel, mechanically spliced as needed with B- and T-series CADWELDS, was used throughout the foundation slab and around the large penetrations. The same type of steel was used for the bonded reinforcing throughout the cylinder and dome as crack control reinforcing and at areas of discontinuities to provide an additional margin of elastic strain capability.

The 1/4"-thick liner plate was attached to the concrete by means of an angle grid system stitch welded to the liner plate and embedded in the concrete. The details of the anchoring system are provided in Figure 5-1. The frequent anchoring is designed to prevent significant distortion of the liner plate during accident conditions and to insure that the liner maintains its leak-tight integrity. The design of the liner anchoring system also considers the various erection tolerances and their effect on its performance. The liner plate was protected from corrosion on the inside with 3 mils of inorganic zinc primer topped with 6 mils of an organic epoxy up to Elevation 75'0", and 3 mils of an inorganic topcoat above that elevation. There is no paint on the side in contact with concrete.

The aggregate used in the structure produced an excellent high-strength, dense, sound concrete. The 28-day design strengths were 5000 psi for the shell and 4000 psi for the foundation slab.

Personnel and equipment access to the structure is provided by a two-door personnel lock with double seals on both doors and by a 19'0" clear diameter, double gasketed, single-door equipment hatch as shown in Figure 5-3. A two-door emergency personnel escape lock is also provided. These locks and hatch were designed and fabricated from A516, Grade 70 firebox quality steel made to A300 specification and Charpy V-notch impact tested to 0°F in accordance with the ASME, B&PV Code, Section III. All piping penetrations furnished adhered to the same requirements.

A containment outage door on the exterior of each Containment Structure at the equipment hatch opening serves as a substitute for the equipment hatch when setting containment closure during Modes 5 and 6 conditions. The containment

outage door was designed, fabricated, examined, inspected and tested to the requirements of the 1995 Edition of ASME Section VIII, Rules for Construction of Pressure Vessels, Division 1. However, the containment outage door cannot be credited for severe weather. If Emergency Response Plan Implementation Procedure 3.0, Preparing for Severe Weather, is implemented and requires containment closure to be established, then the equipment hatch must be used.

Structural brackets provided for the Containment Structure polar crane runway were fabricated from ASTM A36 steel shapes and ASTM A516, Grade 70 insert plates (Figure 5-1). Like the penetration assemblies, structural brackets and thickened plates were shop fabricated, stress relieved and shipped to the job site for welding to the 1/4" liner plate.

The strength of the Containment Structure at working stress and overall yielding was compared to various loading combinations to assure safety. The Containment Structure was examined with respect to strength, the nature and the amount of cracking, the magnitude of deformation, and the extent of corrosion to assure proper performance. The structure was designed and constructed in accordance with design criteria based upon American Concrete Institute (ACI) 318-63, ACI 301-66, and ASME, B&PV Code, Sections III, VIII, and IX to meet the performance and strength requirements prior to prestressing, at transfer of prestress, under sustained prestress, at design loads, and at yield loads.

The structure was originally analyzed using Bechtel's Finite Element Program for Cracking Analysis CE 316-4, for individual and various combinations of loading cases of dead load, live load, prestress, temperature and pressure. The computer output included direct stresses, shear stresses, principal stresses and displacements of each nodal point. See Appendix 5E for an evaluation that reduced the original containment minimum design prestress.

Stress plots which showed the total stresses from appropriate combinations of loading cases were made and areas of high stress were identified. The modulus of elasticity was corrected to account for the nonlinear stress-strain relationship at high compression in these areas and stresses were recomputed.

In order to consider creep deformation, the modulus of elasticity of concrete under sustained loads such as dead load and prestress was differentiated from the modulus of elasticity of concrete under instantaneous loads such as internal pressure and earthquake loads.

The forces and shears were added over the cross-section and the total moment, axial force and shear were determined. From these values, the straight-line elastic stresses were computed and compared to the allowable values. The ACI 318-63 design methods and allowable stresses were used for concrete and prestressed and unprestressed reinforcing steel except as noted in the design criteria.

It is the intent of the criteria to provide a structure of unquestionable integrity that will meet the postulated design conditions with a low strain elastic response. The Calvert Cliffs Containment Structure meets these criteria because: (See Appendix 5E for an evaluation that reduced the original containment minimum design prestress.)

a. The design criteria are in general based on the proven stress and strain to meet the ACI or ASME codes. Departures from or additions to these codes have been made in the following manner:

   1. The environmental conditions of severity of load cycling, weather, corrosion conditions, maintenance, and inspection for this structure have been compared and evaluated with those for code structures to determine the appropriateness of the modifications.
   2. The consultant firm of T.Y. Lin, Kulka, Yang and Associate was retained on earlier projects to assist in the development of design criteria. In addition to assisting with the criteria submitted in the Preliminary Safety Analysis Report, they were involved in the review of design methods to assure that the criteria were implemented as intended.
   3. Dr. Alan H. Mattock of the University of Washington was retained on earlier projects to assist in developing the proper design criteria for combined shear, bending and axial load.
   4. All criteria, specifications and details relating to liner plate and penetrations and corrosion protection have been referred to Bechtel's Metallurgy and Quality Control Department. This department maintains a staff to advise the corporation on problems of welding, quality control, metallurgy and corrosion protection.
   5. The design of the Calvert Cliffs Containment Structure was continually reviewed as the criteria were revised for successive license applications.

b. The primary membrane integrity of the structure is provided by the unbonded post-tensioning tendons, each one of which is stressed to 80% of ultimate strength during installation and performs at approximately 50 to 60% during the life of the structure. Thus, the main strength elements are individually proof-tested prior to operation of the plant.

c. Eight-hundred-seventy-six such post-tensioning elements have been provided, 204 in the dome, and 204 vertical and 468 hoop tendons in the cylinder. Any three adjacent tendons in any of these groups can be lost without significantly affecting the strength of the structure due to the load redistribution capabilities of the shell structure. The bonded reinforcing steel provides for crack control assures that this redistribution capability exists.

d. The unbonded tendons are continuous from anchorage to anchorage, being deflected around penetrations and isolated from secondary strains of the shell. Thus, the membrane integrity of the shell can be assured regardless of conditions of high local strains.

e. The unbonded tendons exist in the structure at a slightly ever-decreasing stress due to relaxation of the tendon and creep of the concrete and, even during pressurization, are subject to a stress change of very small magnitude (2% to 3% of ultimate strength). Thus, the main structural system is never subjected to large changes in load, even during accident conditions.

f. The concrete portion of the structure, similar to the tendons, was subject to the highest state of stress during the initial post-tensioning. During pressurization, it is subject to a large change in load (or state of stress) but the change is, in general, a decrease in load. The large membrane compressive forces are diminished and/or replaced by relatively small radial pressures and stresses.

g. The deformations of the structure during plant operation, or due to accident conditions, are relatively minor due to the low-strain behavior of the concrete. The largest deformations occurred at the time of initial post-tensioning and shortly thereafter, prior to operation. This low strain behavior and the inherent strength of the structure permit the anchoring of all piping penetrating the structure directly to the shell. Such details (Figure 5-2) eliminate the use of expansion bellow seals and significantly reduce the likelihood of leaks developing at the penetrations. The exception to this is when the fuel transfer tube is in use, requiring use of the transfer tube bellows (Section 5.1.4.4.d).

5.1.2.2 Loads

Prior to prestressing, the structure was designed as a conventionally reinforced concrete structure. It is designed for dead load, live loads and a reduced-wind load. Allowable stresses are computed in accordance with ACI 318-63.

Loads at Transfer of Prestress

See Appendix 5E for an evaluation that reduced the original containment minimum design prestress.

The Containment Structure is checked for prestress loads and the stresses compared with those allowed by ACI 318-63 with the following exceptions: ACI 318-63, Chapter 26, allows concrete stress of 0.60 f'_{ci} at initial transfer. In order to limit creep deformations, the membrane compression stress is limited to 0.30 f'_{ci} whereas in combination with flexural compression the maximum allowable stress will be limited to 0.60 f'_{ci} per ACI 318-63.

For local stress concentrations with nonlinear stress distribution as predicted by the finite element analysis, 0.75 f'_{ci} is permitted when local bonded reinforcing is included to distribute and control the localized strains. These high local stresses are present in every structure but they are seldom identified because of simplifications made in design analysis. These high stresses are allowed because they occur in a very small percentage of the cross-section, are confined by material at lower stress and would have to be considerably greater than the values allowed before significant local plastic yielding would result. Bonded reinforcing was added to distribute and control these local strains.

Membrane tension and flexural tension are permitted provided they do not jeopardize the integrity of the liner plate. Membrane tension is permitted to occur during the post-tensioning sequence but will be limited to $\sqrt{f'_{ci}}$. When there is flexural tension but no membrane tension, the section is designed in accordance with the ACI Code, Section 2605(a). The stress in the liner plate due to combined membrane tension and flexural tension is limited to 0.5 f_y.

Shear criteria are in accordance with the ACI 318-63 Code, Chapter 26, as modified by the equations in the structural yielding subsection of this section using a load factor of 1.5 for shear loads.

Loads Under Sustained Prestress

See Appendix 5E for an evaluation that reduced the original containment minimum design prestress.

The conditions for design and the allowable stresses for this case are the same as above except that the allowable tensile stress in unprestressed reinforcing is

limited to 0.5 f_y. ACI 318-63 limits the concrete compression to 0.45 f'_{ci} for sustained prestress load. Values of 0.30 f'_{ci} and 0.60 f'_{ci} are used as described above, which bracket the ACI allowable value. However, with these same limits for concrete stress at transfer of prestress, the stresses under sustained load are reduced due to creep, shrinkage, relaxation, and possible tendon wire breakage. See Appendix 5E for a discussion on possible tendon wire breakage.

At Design Loads

This loading case is the basic "working stress" design. The Containment Structure is designed for the following loading cases:

a. D + F + L (Construction case)
b. D + F + L + T_o + E (Operating case)
c. D + F + L + P + T_A (Design incident case)
d. D + F + L + 1.15P (Test case)
e. D + F + L + T_s + E (Prolonged shutdown case)

D = Dead Load
L = Appropriate Live Load
F = Appropriate Prestressing Load
P = Design Pressure
T_o = Thermal Loads Due to Operating Temperature
T_A = Thermal Loads Corresponding to Pressure P
E = Operating Basis Earthquake (OBE) of 0.08g
T_s = Thermal Loads Due to Transient Wall Temperatures Over a Prolonged Shutdown
(20°F outside face, 50°F inside face)

Sufficient prestressing is provided in the cylindrical and dome portions of the vessel to eliminate membrane tensile stress (tensile stress across the entire wall thickness) under design loads. Flexural tensile cracking is permitted but is controlled by bonded reinforcing steel.

Under the design loads, the same performance limits given for loads at transfer of prestress apply with the following exceptions:

a. If the net membrane compression is below 100 psi, it is neglected and a cracked section is assumed in the computation of flexural bonded reinforcing steel. The allowable tensile stress in bonded reinforcing is 0.5 f_y.

b. When the maximum flexural stress does not exceed $6\sqrt{f'_c}$ and the extent of the tension zone is not more than 1/3 the depth of the section, bonded reinforcing steel is provided to carry the entire tension in the tension block. Otherwise, the bonded reinforcing steel is designed assuming a cracked section. When the bending moment tension is additive to the thermal tension, the allowable tensile stress in the bonded reinforcing steel is 0.5 f_y minus the stress in reinforcing due to the thermal gradient as determined in accordance with the method of ACI-505.

c. The problem of shear and diagonal tension in a prestressed concrete structure should be considered in two parts: membrane principal tension and flexural principal tension. Since sufficient prestressing is used to eliminate membrane tensile stress, membrane principal tension is not critical at design loads. Membrane principal tension due to combined

membrane tension and membrane shear is considered in the next subsection.

Flexural principal tension is the tension associated with bending in planes perpendicular to the surface of the shell and shear stress normal to the shell (radial shear stress). The present provisions of ACI 318-63, Chapter 26 for shear are adequate for design purposes with proper modifications as discussed in the next subsection using a load factor 1.5 for shear loads.

Crack control in the concrete is accomplished by adhering to the ACI-ASCE Code Committee standards for the use of reinforcing steel. These criteria are based upon a recommendation of the Prestressed Concrete Institute and are as follows:

0.25 percent reinforcing shall be provided at the tension face for small members

0.20 percent for medium size members

0.15 percent for large members

A minimum of 0.20% bonded steel reinforcing is provided in two perpendicular directions on the exterior faces of the wall and dome for proper crack control.

The liner plate is attached on the inside faces of the wall and dome. Since, in general, there is no tensile stress due to temperature on the inside faces, bonded reinforcing steel is not necessary there.

Loads Necessary to Cause Structural Yielding

The structure is checked for the factored loads and load combinations that will cause structural yielding.

The load factors are the ratio by which loads will be multiplied for design purposes to assure that the load/deformation behavior of the structure is one of elastic, low-strain behavior. The load factor approach was used in this design as a means of making a rational evaluation of the isolated factors which must be considered in assuring an adequate safety margin for the structure. This approach permits the designer to place the greatest conservatism on those loads most subject to variation and which most directly control the overall safety of the structure. It also places minimum emphasis on the fixed gravity loads and maximum emphasis on accident and earthquake or wind loads. The final design of the structure satisfies the load combinations and factors shown in Appendix 5A.

The load combinations, considering load factors referenced above, are less than the yield strength of the structure. The yield strength of the structure is defined as the upper limit of elastic behavior of the effective load carrying structural materials. For steels (both prestressed and unprestressed) this limit is taken to be the guaranteed minimum yield given in the appropriate ASTM specification. For concrete, it is the ultimate values of shear (as a measure of diagonal tension) and bond per ACI 318-63 and the 28-day ultimate compressive strength for concrete in flexure (f_c'). The ultimate strength assumptions of the ACI Code for concrete beams in flexure are not allowed; that is, the concrete stress is not allowed to go beyond yield.

The maximum strain due to secondary moments, membrane loads and local loads exclusive of thermal loads is limited to that corresponding to the ultimate stress divided by the modulus of elasticity $(f_c'|E_c)$ and a straight-line distribution from there to the neutral axis assumed.

For the loads combined with thermal loads the peak strain is limited to 0.003 in./in. For concrete membrane compression, the yield strength is assumed to be 0.85 f_c' to allow for local irregularities, in accordance with the ACI approach. The reinforcing steel forming part of the load carrying system is allowed to go to, but not to exceed, yield as is allowed for ACI ultimate strength design.

A further definition of yielding is the deformation of the structure which causes strains in the steel liner plate to exceed 0.005 in./in. The yielding of unprestressed reinforcing steel is allowed, either in tension or compression, if the above restrictions are not violated. Yielding of the prestressed tendons is not allowed under any circumstances.

Principal concrete tension due to combined membrane tension and membrane shear, excluding flexural tension due to bending moments or thermal gradients, is limited to $3\sqrt{f_c'}$. Principal concrete tension due to combined membrane tension, membrane shear, and flexural tension due to bending moments or thermal gradients is limited to $6\sqrt{f_c'}$. When the principal concrete tension exceeds the limit of $6\sqrt{f_c'}$, bonded reinforcing steel is provided in the following manner:

a. Thermal Flexural Tension - Bonded reinforcing steel is provided in accordance with the methods of ACI-505. The minimum area of steel provided is 0.20% in each direction.
b. Bending Moment Tension - Sufficient bonded reinforcing steel is provided to resist the bending moment on the basis of cracked section theory using the yield stresses stated above with the following exception: When the bending moment tension is additive to the thermal tension, the allowable tensile stress in the reinforcing steel is f_y minus the stress in reinforcing due to the thermal gradient, as determined in accordance with the methods of ACI-505.

Shear stress limits and shear reinforcing for radial shear are in accordance with ACI 318-63, Chapter 26 with the following exceptions:

Formula 26-12 of the Code was replaced by:

$$V_{ci} = Kb'd\sqrt{f_c'} + M_{cr}\left[\frac{V}{M^1}\right] + V_1$$

where

$$K = \left[1.75 - \frac{0.036}{np'} + 4.0np'\right]$$

but not less than 0.6 for p' ≥ 0.003.

For p' >0.003, the value of K shall be zero.

$$M_{cr} = \frac{I}{Y}\left[6\sqrt{f_c'} + f_{pe} + f_n + f_i\right]$$

f_{pe} = Compressive stress in concrete due to prestress applied normal to the cross-section after all losses (including the stress due to any secondary moment) at the extreme fiber of the section at which tension stresses are caused by live loads.

f_n = Stress due to axial applied loads (f_n shall be negative for tension stress and positive for compression stress).

f_i = Stress due to initial loads at the extreme fiber of a section at which tension stresses are caused by applied loads including the stress due to any secondary moment (f_i shall be negative for tension stress and positive for compression stress).

n = $\frac{475}{\sqrt{f_c'}}$, constant in value of K above

p' = $\frac{As'}{bd}$ ratio of compression steel area to area concrete

V = Shear at the section under consideration due to the applied loads.

M' = Moment at a distance d/2 from the section under consideration, measured in the direction of decreasing moment, due to applied loads.

V_i = Shear due to initial loads (positive when initial shear is in the same direction as the shear due to applied loads).

The lower limit placed by ACI 318-63 on V_{ci} of 1.7 b'd $\sqrt{f_c'}$ is not applied.

Formula 26 -13 of the Code was replaced by:

$$V_{cw} = 3.5b'd(f_c')^{1/2}\left[1 + \frac{f_{pc} + f_n}{3.5\sqrt{f_c'}}\right]^{1/2} + V_p$$

Where V_p = radial shear component of effective prestress due to tendon curvature at the section considered, and the term f_n is as defined above. All other notations are in accordance with ACI 318-63, Chapter 26. It should be noted that this formula is based on the tests and work done by Dr. A. H. Mattock of the University of Washington, and has been included in ACI 318-77, Section 11.5.2.

When the above-mentioned equations show that allowable shear in concrete is zero, radial horizontal shear ties are provided to resist all the calculated shear.

Other Design Loads

The Containment Structure shell is designed for the following loads:

a. Dead load
b. Prestress forces
c. Live load including allowances for piping, ductwork and cable trays
d. Wind, including tornado
e. Earthquake
f. Thermal expansion of pipes attached to the Containment Structure wall
g. Uplift due to buoyant forces

Transients resulting from the LOCA and other lesser incidents are presented in Chapter 14 and serve as the basis for the Containment Structure design pressure of 50 psig and a design concrete surface temperature of 276°F.

The external design pressure of the Containment Structure shell is 3 psig. This value is approximately 0.5 psig beyond the maximum external pressure that could be developed if the Containment Structure were sealed during a period of low barometric pressure and high temperature and, subsequently, the Containment Structure atmosphere was cooled with a concurrent rise in barometric pressure. Vacuum breakers are not provided.

5.1.2.3 Equipment Supports

a. Reactor Vessel Supports

1. Restrain the vessel to maintain the integrity of emergency core cooling systems and to prevent the rupture of additional primary pipes should LOCA occur due to single pipe rupture;
2. Permit slow radial thermal expansion of the vessel under normal operation; and
3. Restrain the vessel against seismic and LOCA jet forces.

b. Steam Generator Supports

1. Restrain the vessel to prevent simultaneous rupture of the primary coolant pipe, and the steam or the feedwater pipes;
2. Permit slow thermal growth of the loops and the vessel; and
3. Restrain all motion under seismic or LOCA loads.

Calvert Cliffs Nuclear Power Plant Units 1 and 2 are approved for leak-before-break based on References 6 and 8, and compliance with Regulatory Guide 1.45 for leak detection as documented in UFSAR Section 4.3.1. As a result of the application of leak-before-break, the mechanical/structural loads associated with the dynamic effects of a large break LOCA in the RCS hot leg or cold legs are no longer considered part of the plant design basis. Accordingly, leak-before-break is credited in the design of the steam generator sliding base supports for the replacement steam generators.

c. Pressurizer Support

1. Support normal operating loads; and
2. Restrain the vessel under seismic loads.

d. Main Coolant Pumps Supports

1. Permit slow thermal movements of the pump; and
2. Restrain the pump under seismic loads.

e. Safety Injection Tank Support

1. Support normal operating loads; and
2. Restrain the tank under seismic loads.

Materials for Equipment Supports

a. Reactor Vessel

1. Plate material	ASTM A302, Gr B
2. Structural shapes	ASTM A441
3. Anchor bolts	ASTM A354, Gr BC
4. Welding electrodes	ASTM A233, E 7018

b. Steam Generator

1. Plate material	ASTM A302, Gr B
2. Anchor bolts	ASTM A490
3. Welding electrodes	ASTM A233, E 7018

c. Pressurizer

1. Anchor bolts	ASTM A354, Gr BC

d. Main Coolant Pump

1. Structural shapes	ASTM A36
2. Machine bolts	ASTM A325
3. Steel plate (S. hangers)	ASTM A515, Gr 65
4. Pipe section (S. hangers)	ASTM A53
5. Machined rod (S. hangers)	AISI C-1015
6. Spring coils (S. hangers)	AISI 4161 H

e. Safety Injection Tank

1. Anchor bolts	ASTM A354, Gr BC

Allowable Stresses and Strain for Equipment Supports Excluding Supports for Piping and Vessels:

a. Stresses under normal operating loads and the OBE are within the applicable code allowable limits.

b. Stresses under combined normal, Safe Shutdown Earthquake (SSE) and accident loads are kept below the yield strength of the material.

c. Allowable local and average strains are determined by the maximum permissible deformation for the support.

5.1.3 CONTAINMENT STRUCTURE DESIGN ANALYSIS

The analysis for the Containment Structure shell falls into two parts, axisymmetric and non-axisymmetric. The axisymmetric analysis is performed through the use of a finite element computer program for the individual loading cases of dead load, live load, temperature, prestress and pressure, as described in Section 5.1.3.1. The axisymmetric finite element representation of the Containment Structure shell does not include the buttresses, penetrations, brackets, and anchors. These items of configuration, the lateral loads due to earthquakes or winds, and various concentrated loads are considered in the non-axisymmetric analysis described in Section 5.1.3.2.

This section includes only analytical techniques, references and design philosophy. The results of these analyses are shown in Section 5.1.4. The design criteria and analysis have been reviewed by Bechtel's consultants, T.Y. Lin, Kulka, Yang and Associate.

5.1.3.1 Axisymmetric Techniques

The finite element technique is a general method of structural analysis in which the continuous structure is replaced by a system of elements (members) connected at a finite number of nodal points (joints). Conventional analysis of frames and trusses can be considered an example of the finite element method. In the application of the method to an axisymmetric solid structure such as the Containment Structure shell, the continuous structure is replaced by a system of rings of quadrilateral cross-section which are interconnected along circumferential joints. Based on energy principles, sets of work equilibrium equations are formed in which the radial and axial displacements at the circumferential joints are the

unknowns. The results of the solution of this set of equations are the deformations of the structure under the given loading conditions. For the output, the stresses are computed knowing the strain and stiffness of each element.

The original finite element mesh used to describe the structure is shown in Figure 5-4 (see Sheets 1 and 2). See Appendix 5E for an evaluation that reduced the original containment minimum design prestress. The upper and lower portions of the structure were analyzed independently to permit the use of a greater number of elements for those areas of the structure of major concern, e.g., the ring girder area and the base of the cylinder. The finite element mesh of the base slab was extended down into the foundation to take into consideration the elastic nature of the foundation material and its effect upon the behavior of the base slab. The tendon access gallery was designed as a separate structure.

The finite element mesh for the Containment Structure does not include the interior structures. The interior structures were included in the finite element input as a lumped mass. The finite element analysis produces stresses due to axisymmetric loads. The stresses from interior structure loads and earthquake loads are superimposed on the finite element stresses. The final summation of all stresses was used to design the base slab, exterior shell and dome. The use of Bechtel's finite element computer program, CE 316-4, permitted an accurate estimate of the stress pattern at various locations of the structure. The major benefit of the program is the capability to predict shears, normal forces and moments due to internal restraint and the interaction of the foundation base slab with the subgrade. The forces and moments were applied to all directions. The following material properties were used in the program for the various loading conditions:

$E_{concrete'}$ Foundation	3.64×10^6 psi
$E_{concrete'}$ Shell	4.07×10^6 psi
$_{concrete}$ (Poisson's Ratio)	0.17
$_{concrete}$ (Coefficient of Expansion)	0.55×10^{-5}
E_{liner}	29×10^6 psi
$F_{y\ liner}$	34,000 psi
E_{soil} (Construction and Operating Case, Figure 5-4, Sheet 1)	
1st Layer	E = 6,200 psi
2nd Layer	E = 9,600 psi
3rd Layer	E = 12,000 psi
E_{soil} (Testing and Accident Case)	
1st Layer	E = 9,600 psi
2nd Layer	E = 14,400 psi
3rd Layer	E = 18,000 psi
E_{soil} (Factored Load-Yield Stress)	
1st Layer	E = 10,000 psi
2nd Layer	E = 20,000 psi
3rd Layer	E = 30,000 psi

In arriving at the above-tabulated values of E, the effect of creep is included by using the following equation for long-term loads such as thermal load, dead load and prestress:

$$E_{cs} = E_{ci} [\xi_i/(\xi_s + \xi_i)],$$

where:

E_{cs} = sustained modulus of elasticity of concrete,

E_{ci} = instantaneous modulus of elasticity of concrete,

ξ_i = instantaneous strain, in./in. per psi, and

ξ_s = creep strain, in./in. per psi

The thermal gradients used in the design are shown in Figure 5-5. The design pressure and concrete surface temperature of 50 psig and 276°F became 75 psig and 276°F at factored conditions.

The compressive stress and strain level is the highest (after the LOCA when the temperature is still relatively high, 200°F, and the pressure is dropping rapidly) at the inside face of the concrete at the edge of openings and also near the liner plate anchors. Neither concentration is a result of what may be considered a real load. In the case of an opening, the real stress is a result of prestress, reduced pressure and dead load. Applying stress concentration factors to these stresses maintains the concrete stress essentially in the elastic range. When the strain and resulting stress from the thermal gradient are also multiplied by a stress concentration factor, the total strain and resulting stress will be above the linear stress range determined by a uniaxial compression test. The relatively high stress level is not of real concern due to the following:

a. The concrete affected is completely surrounded by either other concrete or the penetration nozzle and liner reinforcing plate. This confinement puts the concrete in triaxial compression and gives it the ability to resist forces far in excess of that indicated by a uniaxial compression test.
b. The high state of stress and strain exist at a very localized area and have no effect on the overall containment integrity.

However, to be conservative, reinforcing steel was placed in these areas. The penetration nozzle will also function as compressive reinforcement.

The concrete under the liner plate anchors has some limited yielding in order to get the necessary stress distribution required to resist the liner plate self-relieving loads.

By criteria, yielding was only permitted in the design of the liner plate and of the bonded reinforcing steel for the Containment Structure. Subsequent design analyses, as tabulated in Table 5-1, indicate that the stresses in the liner plate and bonded reinforcing steel will not exceed the allowable yield stresses.

The thermal loads are a result of the temperature gradient across the structure wall. In the finite element analysis, when temperatures are given at every nodal point, stresses are obtained at the center of each element.

The liner plate was handled as an integral part of the structure and was included in the finite element mesh of the Containment Structure, but having different material properties (Figure 5-4, Sheet 1).

Under the LOCA condition or factored load condition, cracking of the concrete at the outside face would be expected. The value of the sustained modulus of elasticity of concrete, E_{cs}, was used in ACI Code 505-54 to find the stresses in concrete, reinforcing steel and liner plate from the predicted design incident thermal loads and factored incident loads.

The method of determining stresses in the concrete and reinforcement required the evaluation of the stress blocks of the cross-section being analyzed.

Stress values were taken from the computer output in the case of axisymmetric loading and from analytical solutions in case of non-axisymmetric loading. Both computations were based on homogeneous materials; therefore, some adjustment was necessary to evaluate the true stress-strain conditions when cracks develop in the tensile zone of the concrete.

An equilibrium equation was written considering the tension force in the reinforcement, the compressive force in the concrete and the axial force acting on the section. In this manner, the neutral axis was shifted from the position defined by the computer analyses to a position which is a function of the amount of reinforcement, the modulus ratio, and the acting axial forces.

The thermal stresses in the containment wall are comparable to those developed in a reinforced concrete slab which is restrained from rotation. The temperature varies linearly across the slab. The concrete will crack in tension and the neutral axis will be shifted toward the compressive extreme fiber. The cracking will reduce the compression at the extreme fiber and increase the tensile stress in reinforcing steel.

The following analysis is based on the equilibrium of normal forces; therefore, any normal force acting on the section must be added to the normal forces resulting from the stress diagram. The effects of Poisson's ratio are considered assuming the reinforcement to be identical in both directions.

Stress-strain relationship in compressed region of concrete:

$$E_c \Sigma_x = \sigma_x - v_c \sigma_y \quad (1)$$

$$E_c \Sigma_y = - v_c \sigma_x + \sigma_y \quad (2)$$

From the above equations (1) and (2):

$$\sigma_x = E_c \frac{\Sigma_x + \Sigma_y V_c}{1 - V_c^2} \quad (3)$$

$$\sigma_\gamma = E_c \frac{\Sigma_\gamma + \Sigma_x V_c}{1 - V_c^2} \quad (4)$$

Substituting,

$\sigma_x = \sigma_y = \sigma_c$ and $\Sigma_x = \Sigma_y = \Sigma_c$ into equations (3) and (4)

$$\sigma_c = E_c \Sigma_c \frac{1}{1 - v_c} = 1.205 E_c \Sigma_c \text{ (if } v_c = 0.17)$$

The reinforcement is acting in one direction, independently from the reinforcement in the perpendicular direction.

Example: If $E_c = 4.07x10^6$ and $E_s = 29x10^6$

$$n_R = \frac{29}{1.205\ x\ 4.07} = 5.9$$

The liner plate is acting in two directions, similar to the concrete except for the difference caused by the Poisson's ratios and elastic modulus:

$$\sigma_L = E_s \Sigma_s \frac{1}{1 - v_L} = 1.35 E_s \Sigma_s, v_L = 0.26$$

$$n_L = \frac{1.35\ x\ 29}{1.205\ x\ 4.07} = 7.98, v_c = 0.17$$

The concrete and reinforcement stresses, due to a moment caused by a loading other than thermal, are calculated by conventional methods. The analysis assumes homogeneous concrete sections. Those concrete and reinforcing steel stresses are then added to the thermal stresses as obtained by the method described above.

Notation:

- E_c Modulus of elasticity of concrete.
- E_s Modulus of elasticity of steel.
- n_L Modular ratio of liner plate-concrete.
- n_R Modular ratio of reinforcement-concrete.
- Σ_c Concrete strain.
- Σ_s Steel strain.
- Σ_x Concrete strain in the X direction.
- Σ_y Concrete strain in the Y direction.
- v_c Poisson's ratio of concrete.
- v_L Poisson's ratio of liner plate.
- σ_c Stress in concrete.
- σ_L Stress in liner plate.
- σ_x Stress in concrete in the X direction.
- σ_y Stress in concrete in the Y direction.

5.1.3.2 Non-axisymmetric Techniques

The non-axisymmetric aspects of configuration or loading required various methods of analysis. The descriptions of the methods used, as applied to different parts of the containment, are given below.

Buttresses

The buttresses and tendon anchorage zones are defined as Seismic Category I elements and were designed in accordance with the general design criteria for the Containment Structure and with the applicable provisions of ACI 318-63, Chapter 26.

The buttresses were analyzed for two effects, non-axisymmetric and anchorage zone stresses.

At each buttress, two out of three hoop tendons are spliced by being mutually anchored on the opposite faces of the buttresses; the third tendon is continuous through the buttress. (The anchors are located on 21-3/4" centers, and are

staggered every 7-1/4" to the opposite face of the buttress. Combined with the continuous tendon, this results in the hoop tendons being positioned at every 7-1/4" along the vertical cross-section of the wall.) Between the opposite anchorages, the compressive force exerted by the spliced tendon is twice as much as elsewhere. This value, combined with the effect of the tendon which is not spliced, will be 1.5 times the prestressing force acting outside of the buttresses. The cross-sectional area at the buttress is about 1.5 times that of the wall, thus the hoop stresses, as well as the hoop strains and radial displacements, can be considered as being nearly constant all around the structure.

The vertical stresses and strains, caused by the vertical post-tensioning, become constant at a short distance away from the anchorages because of the stiffness of the cylindrical shell. The stresses and strains remain nearly axisymmetric despite the presence of the buttresses. The effect of the buttresses on the overall analysis is negligible when the structure is under dead load or prestressing loads.

When an increasing internal pressure acts upon the structure, combined with a thermal gradient such as at the design incident condition, the resultant forces are axisymmetric. The stiffness variation caused by the buttresses will decrease as the concrete develops cracks. The structure will then tend to shape itself to follow the direction of the acting axisymmetric resultant forces even more closely. Thus, the buttress effect is more axisymmetric at yield loads (which include factored pressure) than at design loads including pressure. This fact, combined with the design provision that alternate horizontal tendons terminate in a single buttress, indicates that the buttresses will not reduce the margins of safety available in the structure.

The analysis of the anchorage zone stresses at the buttresses has been determined to be the most critical of all the various types of anchorage areas of the shell. The local stress distribution in the immediate vicinity of the bearing plates has been derived by the following two analysis procedures:

a. The Guyon equivalent prism method: This method is based on experimental photoelastic results as well as on equilibrium considerations of homogeneous and continuous media. It should be noted that the relative bearing plate dimensions are considered.
b. In order to include biaxial stress effects, use has been made of the experimental test results presented by S. J. Taylor at the March 1967 London Conference of the Institution of Civil Engineers (Group H, Paper 49). This paper compares test results with most of the currently used approaches (such as Guyon's equivalent prism method). It also investigates the effect of the rigid trumpet welded to the bearing plate.

The Guyon method yields the following results:

Maximum compressive stress under the bearing plate,

σ_c = -2400 psi

Maximum tensile stress in spalling zone,

$\sigma_{spalling}$ = +2400 psi = - σ_c

Maximum tensile stress in bursting zones,

$\sigma_{maximum\ bursting}$ = (0.04) x avg. stress = +96 psi

S. J. Taylor's experimental results indicate that the anchor plate will give rise to a similar stress distribution pattern as Guyon's method; the main difference lies in

the fact that the central bursting zone has a tensile stress peak of twice Guyon's value:

$\sigma_{\text{maximum bursting}}$ = +192 psi

A state of biaxial tension in the concrete will appear on the outside face under the loading case 1.05D + 1.5P + 1.0T_A + 1.0F. The superposition of the corresponding state of stress with the local anchor stresses reduces the load carrying capacity of the anchorage unit and causes a reduction in the maximum tensile strain to cracking.

On the other hand, the uniform compressive state of stress (vertical prestress) applied to the anchorage zone increases the load carrying capacity of the anchorage unit, with the maximum tensile strain to cracking being increased.

The design of the buttress anchor zones considered such additional vertical stresses, leading to a state of pseudo biaxial stress, the second direction being radial through the thickness.

For the above-mentioned case, i.e., 1.05D + 1.5P + 1.0T_A + 1.0F, the averaged vertical (meridional) stress component is:

$f_a \simeq$ + 400 psi

The compressive bearing plate stress at 10" depth below the bearing plate is:

fc $\simeq$ - 1500 psi

Thus, the two values introduced in the biaxial stress envelopes proposed in S. J. Taylor's article are:

f_c/f_c' = 1500/5000 = 0.3
$f_c//f_c'$ = 400/5000 = 0.08

These values show that failure could occur if vertical reinforcing was not provided. In fact, the maximum allowable vertical average tensile stress according to Taylor's interaction curve is f_a/f_c' = 0.03, therefore f_a = +150 psi.

The three-dimensional stress distribution in the anchor zones was analyzed in sufficient detail to permit the rational evaluation of stress concentrations. A conical wedge segment was used as the basic design element and the radial splitting tension was determined as a tangential distribution function. The summation of splitting stresses through the entire volume of the lead-in zone established the value of the splitting force. This force is a function of the a/b ratio and the cone angle and/or, a/b and h. Several different combinations of the values were analyzed and the most critical values selected. A system analysis for the vertical splitting force was carried out based on statics. The magnitude of vertical and spalling forces were also determined.

The most unfavorable loads and load combinations were considered in the analysis of the anchorage zone. Stresses based on transient thermal gradients were used in all cases where the use of a steady state gradient underestimated the stresses and strains and were superimposed on the bursting stresses determined from the triaxial stress calculations. The computed stresses are less than the ACI allowable values. The design of the concrete reinforcement is based on this conservative analysis to provide a margin of safety similar to the other components of the reactor building structure and to control cracking in the

anchorage zone. As a result, there is no danger of delayed rupture of the concrete under sustained load due to local overstress and microcracking.

The reinforcing details, including the method for anchoring and splicing the reinforcing, are shown on Figure 5-1.

The reinforcement required has been designed primarily to resist tensile forces, and has been located such that it will efficiently do so. The reinforcement was provided for load cases which create the maximum tensile forces and for other load cases the relevant shear forces or stresses were superimposed.

The amount of reinforcing steel was computed manually for all Seismic Category I structures, except the exterior shell and the base slab of the Containment Structure, using conventional reinforced concrete design methods for "Working Stress Design" and "Ultimate Strength Design" depending on the governing load combination.

The seismic analysis was conducted as described in the following subsection, providing values for lateral accelerations, shears, moments and displacements at specified locations. The lateral acceleration values are applied to the axisymmetric Containment Structure as non-axisymmetric static loading in Bechtel's Analysis of Axisymmetric Shell and Solid Subject to Non-Axisymmetric Static Loading, Dynamic Loading or Base Acceleration Program, CE 771. The Containment Structure is idealized as an assemblage of a series of discretized elements. Resultant shear forces, longitudinal, circular and cross moments are calculated from stresses obtained as an output from program CE 771 at 15° increments, from 0° to 180° and at 270°. The combined shear forces, normal forces, and moments are applied to the specified section and, using crack section analysis and compressive and tensile stresses in concrete, liner plate interior and exterior reinforcement are determined. Allowable working case stress and yield case stress determine the required area of reinforcement in the specified section.

The possibility of the concrete breaking along shear planes was considered at the intersection of (1) the buttress with the cylinder and (2) the cylinder with the base slab.

a. Buttress - Cylinder Intersection

   An increase in the compression force at the buttress corresponds to an increase in the concrete area of the same magnitude.

b. Cylinder - Base Slab Intersection

   An analysis for the most critical radial shear conditions was performed. The difference in shear stiffness between the shell and the buttress and the remainder of the shell was included as a shear amplification factor. The reinforcing required was less then the reinforcing provided.

The possibility of concrete breaking along a shear plane is excluded by providing ample reinforcing. In other locations, breakage along the shear plane has been excluded by the opposition of prestressing and anchor forces.

For this reason, special anchorage zone reinforcing is based on the following considerations:

a. Full-scale load tests and final designs of similar anchorages.

b. The post-tensioning supplier's recommendations of anchorage reinforcing requirements.
c. Review of the final details of the combined reinforcing on earlier projects by the consulting firm of T.Y. Lin, Kulka, Yang and Associate.

Seismic or Wind Loading

Seismic loading of the structure is higher in all cases than that of tornado or wind loading. The seismic analysis was conducted in the following manner:

The loads on the Containment Structure caused by earthquake were determined by a dynamic analysis of the structure. The dynamic analysis was made on an idealized structural model of lumped masses and weightless elastic columns acting as springs.

The analysis consists of three steps:

(1) The determination of the natural frequencies of the structure and its mode shapes, (2) the response of these modes to the earthquake by the response spectrum technique, and (3) combining modal responses to obtain structural response.

The natural frequencies and mode shapes were computed using the matrix equation of motion shown below for a lumped mass system. The form of the equation is:

$$\omega_n{}^2[m]\{\phi_n\} = [K]\{\phi_n\}, \text{ where}$$

[K] = matrix of stiffness coefficients including the combined effects of shear and flexure in the structure and the rotation, and horizontal translation of the base slab on soil.

[m] = matrix of concentrated masses.

$\{\phi_n\}$ = matrix of mode shapes

ω_n = angular frequency of vibration in the n-th mode.

The results of this computation are the several values of ω_n for n and mode shapes ϕ_n = 1, 2, 3,….p, where p is the total number of degrees of freedom (i.e., lumped masses) in the idealized model.

The response of the structure to the specified earthquake was then computed by the response spectrum technique as follows:

a. Using mode frequencies and respective damping values, a response acceleration, S_n, is read from the spectrum curves for each mode.

The modal acceleration, A_n, is given by:

$$A_n = S_n \frac{\sum_{i=1}^{P} \emptyset_{in} m_i}{\sum_{i=1}^{P} \emptyset_{in}^2 m_i}$$

The acceleration per point i and per mode n is given by:

$A_{in} = \phi_{in} A_n$

The inertial force per point per mode, F_{in}, is given by:

$$F_{in} = m_i A_n$$

where m_i is the mass lumped at point i.

b. Using the inertial force per point per mode, F_{in}, shears and moments are computed per point per mode. The "Root Mean Square" method is used for combining modal responses (shears, moments, stresses, deflections, and/or accelerations) in the response spectrum modal analysis of Seismic Category I structures. In this method, responses are combined using the square root of the sum of the squares of responses of each mode. This method was for combining all predominant modal responses including closely spaced modal frequencies. We have examined the effect of adding closely spaced modes linearly, and find that allowable stresses have not been exceeded.

c. Seismic and wind shears are transferred across construction joints either by friction, by bond, by shear keys or by a combination of these.

Large Openings (Equipment Hatch and Personnel Lock Opening)

The primary loads considered in the design of the equipment hatch and personnel lock opening, as in any other part of the structure, were dead load, prestress, pressure, earthquake, and thermal loads. The secondary loads considered were the following effects caused by the above primary loads:

The deflection of tendons around the opening;

The curvature of the shell at the opening; and

The thickening around the opening.

The primary loads listed are mainly membrane loads with the exception of the thermal loads. In addition to membrane loads, incident pressure also produces punching shear around the edge of the opening. The magnitudes of these loads for design purposes were the magnitudes at the center of the opening. These are fairly simple to establish knowing the values of hoop and vertical prestressing, incident pressure, and the geometry and location of the opening.

Secondary loads were computed by the following methods:

a. The membrane stress concentration factors and effect of the deflection of the tendons around the equipment hatch were analyzed for a flat plate by the finite element method. The stresses computed by conventional stress concentration factors, compared with those values found from the above-mentioned finite element computer program, demonstrated that the deflection of the tendons does not significantly affect the stress concentrations. This is a plane stress analysis and does not include the effect of the curvature of the shell. However, it gives assurance of the correctness of the assumed membrane stress pattern caused by the prestressing around the opening.

b. With the help of Reference 1, stress resultants around the large opening were found for various loading cases. Comparison of the results found from this reference with the results of a flat plate of uniform thickness with a circular hole, showed the effect of the cylindrical curvature on stress concentrations around the opening.

Normal shear forces (relative to the opening) were modified to account for the effect of twisting moments (Reference 1). These modified shear forces are called Kirschoff's shear forces. Horizontal wall ties were provided to resist a portion of these shear forces.

c. The effect of the thickening on the outside face around the large opening was investigated using several methods. Reference 2 was used to evaluate the effect of thickening on the stress concentration factors for membrane stress. A separate axisymmetric finite element computer analysis, for a flat plate with thickening on the outside face, was prepared to handle both axisymmetric and non-axisymmetric loads. This program predicts the effect of the concentration of hoop tendons with respect to the Containment Structure at the top and bottom of the opening.

   For the analysis of the thermal stresses around the opening, the same method was used as for the other loadings. At the edge of the opening, a uniformly distributed moment, equal but opposite to the thermal moment existing on the rest of the shell, was applied and evaluated using the methods of the preceding Reference 1. The stresses were then superimposed on the stresses calculated for the other loads.

   In the case of LOCA temperature, after the incident pressure has already decreased, very little or no tension develops on the outside, so thermal strains will exist without the relieving effect of the cracks. However, the liner plate will reach a high strain level and so will the concrete at the inside corner of the penetrations, thereby relieving the very high stresses, but still carrying a high moment in the state of redistribution stresses.

   In the case of 1.5P (prestress fully neutralized) + $1.0T_A$ (accident temperature), the cracked concrete, with highly strained tension reinforcement, constitutes a shell with stiffness decreased but still essentially constant in all directions. See Appendix 5E for an evaluation that reduced the original containment minimum design prestress. In order to control the increased hoop moment around the opening, the hoop reinforcement is about twice that of the radial reinforcement (Figure 5-3).

The equipment hatch opening was thus thickened for the following reasons:

1. To reduce the predicted high membrane stresses around the opening;
2. To facilitate tendon placement;
3. To facilitate steel reinforcing placement; and
4. To compensate for the reduction in the overall shell stiffness due to the opening.

Since the resultant forces on any part of the containment exterior structure produce compressive stresses in the concrete, and sufficient unprestressed reinforcement is provided to control any local cracking, no significant cracks are expected. In the absence of any significant cracks, it is believed that the concrete will provide adequate corrosion protection for the liner plate. Cathodic protection for the Containment Structure is described in Section 5.1.7. Thus, no surveillance measures are necessary to detect the corrosion of the liner plate in the Containment Structures.

The working stress method, i.e., elastic analysis, was applied to both load combinations for design loads, as well as for yield loads, using the analytical

procedures described above. The only difference is the higher allowable stresses under yield conditions. The various factored load combinations and capacity reduction factors are specified in Appendix 5A and were used for the yield load combinations using the working stress design method. The design assumption of straight line variation of stresses was maintained under yield conditions.

The governing design condition for the edges of the equipment hatch opening at the outside face is the LOCA. Under this condition, approximately 60% of the total bonded reinforcing steel needed at the edge of the opening at the outside face, is required to resist the thermal load.

Excluding the thermal load, the remaining stress, equivalent to approximately 40% of the total stress including thermal, at the edge of the outside face, is the sum of the following stresses:

Normal stresses, resulting from membrane forces, including the effect of thickening, contribute approximately minus 45% (minus 18% of the total).

Flexural stresses, resulting from the moments caused by thickening on the outside face, contribute approximately 155% (62% of the total).

Normal and flexural stresses, resulting from membrane forces and moments caused by the effect of cylindrical curvature, contribute approximately minus 10% (minus 4% of total).

Penetrations

Analysis of the Containment Structure penetrations was divided into three parts: (1) the concrete shell, (2) the liner plate reinforcement and closure to the pipe, and (3) the thermal gradients and protection requirements at the high-temperature penetrations. The three parts will be discussed separately.

a. Concrete Shell

In general, special design consideration was given to all openings in the Containment Structure. Analysis of the various openings has indicated that the degree of attention required depends upon the penetration size. Small penetrations are considered to be those with a diameter smaller that 2-1/2 times the shell thickness, i.e., approximately 8' in diameter or less. For openings of 8' diameter or less, the curvature effect of the shell is negligible (Reference 1). In general, the typical concrete wall thickness has been found to be capable of taking the imposed stresses using bonded reinforcement, and the thickness is increased only as required to provide space requirements for radially deflected tendons. The induced stresses, due to normal thermal gradients and postulated rupture conditions, distribute rapidly and are of a minor nature compared to the numerous loading conditions for which the shell must be designed. The small penetrations are analyzed as holes in a flat plate. Applied piping restraint loads due to thermal expansion or accident forces are assumed to distribute in the cylinder as stated in Reference 3. Typical details associated with these opening are indicated in Figure 5-2.

b. Liner Plate Closure

The stress concentrations around openings in the liner plate were calculated using the theory of elasticity. The stress concentrations were then reduced by the use of a thickened plate around the opening. In the case of a penetration with no appreciable external load, shear connectors were used to maintain deformation compatibility between the liner plate

and the concrete. Inward displacement of the liner plate at the penetration was also controlled by shear connectors.

In case significant external operating loads are imposed upon the pipe penetration, the stress level from the external loads is limited to the design stress intensity values, S_m, given in the ASME, B&PV Code, Section III, Article 4. The stress level in the shear connectors from external loads is in accordance with American Institute of Steel Construction (AISC) Code for A-36 steel.

The combining of stresses from all effects was performed using the methods outlined in the ASME, B&PV Code, Section III, Article 4, Figure N-414. Figure 5-9 shows a typical penetration and the applied loads.

Stresses due to the effects of pipe loads, pressure loads, dead loads, and earthquake loads were calculated and the stress intensity was kept below S_m.

The stresses from the remaining effects were combined with the above-calculated stresses and the resultant stress intensity kept below S_a.

c. Thermal Gradient

The only high temperature pipes penetrating the Containment Structure shell are the main steam and feedwater pipes, steam generator blowdown line, and the reactor coolant letdown and sampling lines. Cooling was provided to maintain the temperature in these penetrations below 150°F.

Liner Plate

The primary purpose of the liner plate (including welds) is to provide leak tightness integrity to the post-tensioned concrete containment. Structural integrity of the structure is provided by the post-tensioned concrete and not by the liner plate.

The design, construction, inspection, and testing of the liner plate, which acts as a membrane and is not a pressure vessel, was not covered by any recognized code or specification. All components of the liner that must resist the full design pressure, such as penetrations, were selected to meet the requirements of ASME, B&PV Code, Section III, Nuclear Vessels, Paragraph N-1211. ASTM A516, Grade 60 or 70 made to ASTM A300 is a steel which meets these requirements and thus was used as a plate material for penetrations. This material has excellent weldability characteristics.

There are no design conditions under which the liner plate is relied upon to assist the concrete in maintaining the integrity of the structure, even though the liner may provide assistance in order to maintain deformation compatibility.

Loads are transmitted to the liner plate through the anchorage system and through direct contact with the concrete and vice versa. At times, loads may also be transmitted by bond and/or friction with the concrete. These loads cause, or are caused by, liner strain. The liner was designed to withstand the predicted strains.

Possible cracking of concrete has been considered and reinforcing steel is provided to control the width and spacing of the cracks. In addition, the design is such that total structural deformation remains small during the loading conditions, and that any cracking will be orders of magnitude less than that sustained in the repeated attempts to fail the prestressed concrete reactor vessel "Model 1," and

even smaller than the concrete strains of overpressure tests of "Model 2" (both at Gulf-General Atomic) (References 4 and 5).

As described, the consequences of concrete cracking on structural integrity are limited by the bonded reinforcing and unbonded tendons that have been provided. The effect of concrete cracking on the liner plate has also been considered. The anchor spacing and other features are such that the liner will sustain orders of magnitude of strain less than did the liner of Model 1 at Gulf-General Atomic (Reference 4) without tensile failure.

Liner Plate Anchors

The liner plate anchors were designed to preclude failure when subjected to the worst possible loading combinations. The anchors were also designed such that, in the event of a missing or failed anchor, the total integrity of the anchorage system would not be jeopardized.

The following loading conditions were considered in the design of the anchorage system:

Prestress
Internal Pressure
Shrinkage and Creep of Concrete
Thermal Gradients
Dead Load
Earthquake Loading
Wind or Tornado Loadings
Vacuum

The following factors were also considered in the design of the anchorage system:

Initial inward curvature of the inner plate between anchors due to fabrication and erection inaccuracies.
Variation of anchor spacing.
Misalignment of liner plate seams.
Variation of plate thickness.
Variation of liner plate material yield strength.
Variation of Poisson's ratio for liner plate material.
Cracking of concrete in anchor zone.
Variation of the anchor stiffness.

The anchorage system satisfies the following conditions:

The system has sufficient strength and ductility, with energy absorbing capability sufficient to restrain the maximum force and displacement resulting from the condition where a panel with initial outward curvature is adjacent to a panel with initial inward curvature.
The system has sufficient flexural strength to resist the bending moment which would result from the above condition.
The system has sufficient strength to resist any radial pull-out forces.

Liner Supports

In designing for structural bracket loads applied parallel to the plane of the liner plate, or loads transferred through the thickness of the liner plate, the following criteria and methods have been used:

The liner plate was thickened to reduce the predicted stress level. The thickened plate, with the corresponding thicker weld attaching the bracket to the plate, will also reduce the probability of the occurrence of a leak at this location.

For tensile loads applied perpendicular to the plane of the liner plate, sufficient anchorage is provided.

The allowable stress in the perpendicular direction was calculated using the allowable predicted strain in that direction together with the predicted stresses in the plane of the liner plate.

In setting the above criteria, the reduced strength and strain capability of the material, perpendicular to the direction of rolling, was also considered. In this case, the major stress is normal to the plane of the thickened liner plate. The allowable stresses were reduced to 75% of the allowable stress calculated above.

5.1.4 IMPLEMENTATION OF CRITERIA

See Appendix 5E for an evaluation that reduced the original containment minimum design prestress.

This section documents the manner in which the design criteria were met by the designer.

Section 5.1.4.1 discusses original isostress plots and tabulations of predicted stresses for various materials. The isostress plots of the homogeneous cracked concrete structure indicate the general stress pattern for the structure as a whole, under various loading conditions. More specific documentation is made of the predicted stresses for all materials in the structure. In these tabulations, the predicted stresses are compared with the allowable to permit an easy comparison and evaluation of the adequacy of the design.

Sections 5.1.4.3 and 5.1.4.4 illustrate the actual details used in the design to implement the criteria.

5.1.4.1 Results of Analysis

See Appendix 5E for an evaluation that reduced the original containment minimum design prestress.

The isostress plots, Figures 5-6 and 5-7, show the three principal stresses and the direction of the principal stresses normal to the hoop direction. The principal stresses are the most significant information about the behavior of the structure under various conditions and were a valuable aid for the final design.

The plots were prepared by a cathode-ray tube plotter. The data for plotting were taken from the stress output of the finite element computer program of the following load cases:

D + F + L (Construction Case)
D + F + L + 1.15P (Test Case)

$D + F + L + P + T_A$ (Design Incident Case)

$\frac{1}{\phi}$ (1.05 D + F + 1.5P + T_A) (Factored Load Case)

The above axisymmetric loading conditions have been found to be governing in the design since they result in the highest stresses at various locations in the structure.

The containment stress analysis results for structural concrete and liner plate, including shear stresses, are shown here.

5.1.4.2 Prestress Losses

See Appendix 5E for a discussion on possible prestress losses due to tendon wire breakage.

In accordance with ACI Code 318-63, the original design provided for prestress losses caused by the following effects:

a. Seating of anchorage;
b. Elastic shortening of concrete;
c. Creep of concrete;
d. Shrinkage of concrete;
e. Relaxation of prestressing steel stress; and
f. Frictional loss due to intended or unintended curvature in the tendons.

All of the above losses can be predicted with sufficient accuracy.

In this case, the environment of the prestress system and concrete is not appreciably different from that found in numerous bridge and building applications. Considerable research has been done to evaluate the above items and is available to designers in assigning the allowances. Building code authorities consider it acceptable practice to develop permanent designs based on these allowances.

The following categories and values of prestress losses have been considered in the design:

Type of Loss[(a)]	Assumed Value
Seating of Anchorage	None
Elastic Shortening of Concrete	2 ksi
Shrinkage and Creep of Concrete for	
Dome tendons (test data)	146.7×10^{-6} in./in.
Hoop tendons (test data)	248×10^{-6} in./in.
Vertical tendons (test data)	137.5×10^{-6} in./in.
Relaxation of Prestressing Steel(b)	9.5% of 0.70 f_s' = 15.96 ksi
Frictional Loss	K = 0.0003, μ = 0.158

(a) See Appendix 5E for a discussion on possible prestress losses due to tendon wire breakage.

(b) See Appendix 5E for a discussion on the relaxation value of the prestressing steel used for vertical tendons replaced in 2001 through 2002 on both Units.

There is no allowance for the seating of the BBRV anchor since no slippage occurs in the anchor during transfer of the tendon load into the structure. Sample lift-off readings will be taken to confirm that any seating loss is negligible.

The loss of tendon stress due to elastic shortening was based on the change in the initial tendon relative to the last tendon stressed.

The value used for shrinkage and creep loss represents only that which could occur after stressing. In general, since the concrete is well aged at the time of stress, little shrinkage and creep is left to occur and add to prestress loss.

The value of relaxation loss is based on the information furnished by the tendon system vendor, The Prescon Corporation. See Appendix 5E for a discussion on the relaxation value of the prestressing steel used for vertical tendons replaced in 2001 through 2002 on both Units.

Frictional loss parameters for unintentional curvature (K) and intentional curvature (μ) are based on full-scale friction test data. This data indicates actual values of K = 0.0003 and μ = 0.125 versus the design values of K = 0.0003 and μ = 0.158.

Assuming that the jacking stress for the tendons is 0.80 f_s' or 192,000 psi and using the above prestress loss parameters, the following tabulation shows the magnitude of the design losses and the final effective prestress at the end of 40 years for a typical dome, hoop, and vertical tendon. See Appendix 5E for a discussion on the relaxation value of the prestressing steel used for vertical tendons replaced in 2002 through 2002 on both Units, and a discussion on the final effective prestress at the end of 60 nominal years due to license extension.

	Dome[c] (ksi)	Hoop[c] (ksi)	Vertical[c] (ksi)
Jacking Stress	192	192	192
Friction Loss	20.86	29.6(a)	21.7
Seating Loss	0	0	0
	171.14	162.4	170.3
Elastic Loss	2.0	2.0	2.0
Creep and Shrinkage Loss	4.26	7.19	3.98
Relaxation Loss	15.96	15.96	15.96
Final Effective Prestress(b)	148.92	137.25	148.36

(a) Average of crossing tendons.

(b) This force does not include the effect of pressurization, which increases the prestress force.

(c) Losses shown are for original nominal 40-year license. See Appendix 5E for a discussion of losses at the end of 60 nominal years due to the license extension.

To provide assurance of achievement of the desired level of final effective prestress and that ACI 318-63 requirements were met, a written procedure was prepared for guidance of post-tensioning work. The procedure provided nominal values for end anchor forces in terms of pressure gauge readings for calibrated jack-gauge combinations. Force measurements were made at the end anchor since that is the only practical location of such measurements.

The procedure required the measured temporary jacking force for a single tendon to approach, but not exceed 850 kips (0.8 f_s'). Thus the limits set by ACI 318-63 2606(a)1, and of the prestressing system supplier, were observed. Additionally, benefits were obtained by in-place testing of the tendon to provide final assurance that the force capability exceeded that required by design. During the increase in force, measurements were required of elongation changes and force changes in order to allow documentation of compliance with ACI 318-63 2621(a). The procedure required that the prestressing steel be installed in the sheath before stressing for a sufficient time period that the temperatures of the prestressing steel and concrete reach essential equilibrium, to establish conformance with ACI 318-63 2621(e). The jacking force of 0.8 f_s' further provided for a means of equalizing the force in individual wires of a tendon to establish compliance with ACI 318-63 2621(b). The procedures required compliance with ACI 318-63 such that, if broken wires resulted from the post-tensioning sequence, compliance with Section 2621(d) was documented. Each of the above procedures contributed to assurance that the desired level of final effective prestress would be achieved.

Paragraph 2606(a)2 of ACI 318-63 refers to "tendons" rather than to an individual tendon. Further, the paragraph does not refer to the location to be considered for the determination of 0.8 f_s', for example, "temporary jacking force" referred in paragraph 2606(a)1.

Two interpretations were required; both had to consider the effect of the resultant actions on both the prestressing system and structure.

The first interpretation was that the location for measurement of the seating force, used in calculating the percentage of f_s', was at the end anchor and just subsequent to the measurement of the "temporary jacking force" referred in ACI 2606(a)1. The advantages of this location are several. One is that it is a practical one and thus the possibility for achieving valid measurements is greater. The second is that it is the same location used for measuring the "temporary jacking force" and measurements could be made without the added complexity of additional measuring devices. The third advantage is that measurements at this location provide assurance that the calculated percentage of f_s' at seating does not anywhere exceed the maximum percentage of f_s' to which that tendon has been subjected.

Several possible cases were considered for the second interpretation so as to allow anchoring of an individual tendon without exceeding the requirement stated for "tendons" collectively in ACI 318-63 2606(a)2. One such case assumed that the anchoring force for the typical tendon was that for a tendon anchored midway through the prestressing sequence. It further assumed that the losses to be assumed were one-half of the sum of elastic losses, and of the creep, shrinkage, and relaxation predicted to occur during the entire prestressing sequence. This interpretation, however, was considered to be neither practical nor enforceable, since it resulted in changing the seating forces as the actual (as compared to the schedule) time length of the prestressing period was dictated by weather and manpower availability.

In another case, the stressing is done by jacking each tendon to the required force of 850 kips (0.8 f_s'), and placing shims of predetermined thickness, corresponding to the calculated elongation, between the bearing plate assembly and the washer. Proper tendon stress is assured by comparing the jack pressure and tendon elongation with previously calculated values.

The case adopted was to seat each tendon with a measured "pressure" reading for the jack, at "lift-off" of the end anchor, of 775 kips (between 0.72 and 0.73 f_s',). This procedure had several advantages.

One advantage was that the force on the containment and the tendon was within the bounds of those for which it had been tested and resulted in no known detrimental effects. The second advantage was that the stressing procedure was simplified, since the stressing crews did not have to accommodate a large number of different anchoring force requirements. The third advantage was that, at the completion of stressing the last tendon, the expected losses were such that the average percentage of f_s' at the end anchors of the tendons would be less than 0.7 f_s' thus establishing compliance with ACI 318-63 2606(a)1 and 2. The fourth advantage was that the percentage loss of prestressing force was less than would be the case if the tendons were anchored in such a manner that the calculated percentage of f_s' nowhere exceeded 0.7 f_s'.

The latter advantage deserves special mention since it plays a strong role in assuring that the final effective prestress equaled or exceeded the desired value. For example, if the percentage of f_s' at the anchorage of the tendons were 0.1 f_s', creep and shrinkage of concrete could result in the loss of almost all of the prestressing force. Assuming that the total losses due to creep, shrinkage and elastic shortening equal 0.1 f_s', then the final effective prestress would be 20% of an initial prestress equivalent to 0.5 f_s'. If the initial prestress was equivalent to 0.7 f_s', the final effective prestress, neglecting relaxation for the moment, would be about 86% of the initial prestress. Clearly, the assurance (that the concrete creep and shrinkage losses have been properly accounted for) increases as the percentage of f_s' for the anchored tendon(s) increases. However, this design was committed to meeting the ACI 318-63 requirement and the anchorage force for the tendons was kept at or below 0.7 f_s' in accordance with the interpretation described.

5.1.4.3 Liner Plate

The following design bases were applied to the containment liner so that it meets the specified leak-rate under LOCA conditions:

a. The liner is protected against damage by missiles. (Section 5.1.5.3)
b. The liner plate strains are limited to allowable values that have been shown to result in leak-tight vessels or pressure piping.
c. The liner plate is prevented from development of significant distortion.
d. All discontinuities and openings are properly anchored to accommodate the forces exerted by the restrained liner plate, and careful attention is paid to details of corners and connections to minimize the effects of discontinuities.

Pressure vessels, pressure piping, high pressure hydraulic tubing, and similar containers are made by cold forming, drawing, and dishing operations, where strains may approach the elongation capacity of the material. (For mild steel at failure, this elongation varies from 15 to 30%.) These forming operations result in high strains both in tension and compression. Vessels and piping components manufactured by these methods have a history of high leak-tight integrity, proving that subjecting the steel material to high strain does not affect its leak-tight integrity.

The best basis for establishing allowable liner plate strains is considered to be that portion of the ASME, B&PV Code, Section III, Nuclear Vessels, Article 4.

Specifically, the following sections have been adopted as guides in establishing allowable strain limits:

Paragraph N-412(m)	Thermal Stress
Paragraph N-414.5	Peak Stress Intensity
Table N-413	Classification of Stresses for Some Typical Cases
Figure N-414	Stress Categories and Limits of Stress Intensity
Figure N-415(A)	Design Fatigue Curves
Paragraph N-412(n)	Operational Cycle
Paragraph N-415.1	Vessels Not Requiring Analysis for Cyclic Operation

American Society of Mechanical Engineers design codes require that the liner material be prevented from experiencing significant distortion due to the thermal load and that the stresses be considered from a fatigue standpoint [Paragraph N-412(m)(2)]. The following fatigue loads were considered in the design of the liner plate:

a. Thermal cycling due to annual outdoor temperature variations. Daily temperature variations do not penetrate a significant distance into the concrete shell to appreciably change the average temperature of the shell relative to the liner plate. The original number of cycles for this loading is 40 cycles for the plant life of 40 years. Reference 10 provides an evaluation of the effect of thermal cycling on the liner plate for a total of 60 years. The evaluation concluded that the containment liner plate is acceptable for 60 years.

b. Thermal cycling due to interior temperature variations during the startup and shutdown of the reactor system. The number of cycles for this loading was assumed to be 500.

c. Thermal cycling due to the LOCA was taken very conservatively to occur only once during plant life. Thermal load cycles in the piping systems are somewhat isolated from the liner plate penetrations by the concentric sleeves between the pipe and the concrete. The attachment sleeve was designed in accordance with ASME, B&PV Code, Section III fatigue considerations. All penetrations were reviewed for a conservative number of cycles to be expected during plant life.

Thermal stresses in the liner plate fall into the categories considered in Article 4, Section III, Nuclear Vessels of the ASME, B&PV Code. The allowable stress in Figure N-415(A) is for alternating stress intensity for carbon steels and temperatures not exceeding 700°F. In addition, the ASME code further requires that significant distortion of the material be prevented.

In accordance with ASME, B&PV Code, Paragraph 412(m)(2), the liner plate is restrained against significant distortion by continuous angle anchors and never exceeds the temperature limitation of 700°F. It also satisfies the requirements for limiting strains on the basis of fatigue consideration. A typical section showing the anchors is included in Figure 5-1.

American Society of Mechanical Engineers, B&PV Code, Paragraph 412(n), Figure N-415(A), has been developed as a result of research, industry experience, and the proven performance of code vessels. Because of the conservative factors it contains on both stress intensity and stress cycles, and its being a part of a recognized design code, Figure N-415(A) and its appropriate limitations have been used as a basis for establishing allowable liner plate strains. Since the graph in

Figure N-415(A) does not extend below ten cycles, ten cycles was used for the LOCA instead of one cycle mentioned above.

Establishing an allowable strain based on ten significant thermal cycles of the LOCA condition would permit an allowable strain [from Figure N-415(A)] of approximately 2%. Maximum allowable tensile or compressive strain has been conservatively set at 0.5% (compared to 2% shown above). The maximum predicted strain in the liner plate during LOCA conditions has been found to be 0.25% compression.

At the design LOCA condition, there will be no tensile stress anywhere in the liner plate membrane. This is true both at the time of initial pressure release and under any later pressure and temperature condition. The purpose of specifying a non-destructive examination temperature requirement is to provide protection against a brittle fracture or cleavage mode of failure. However, this type of failure is precluded by the absence of tensile stresses.

No allowable compressive strain value has been set for the test condition because the value will be less than that experienced under the LOCA condition. The maximum allowable tensile strain will be 0.2% under test conditions; the predicted value is much smaller.

The maximum compressive strains are caused by LOCA pressure, thermal loading prestress, shrinkage, and creep. The maximum calculated strains do not exceed 0.0025 in./in. and the liner plate will always remain in a stable condition.

The stability of the liner plate has been studied for the loading cases and deformations to which it may reasonably be subjected. The critical loading cases that were considered included the LOCA condition and the operating condition during the winter.

Two separate solutions to the plate stability problem were made:

a. As a compressed panel under biaxial compression, assuming that the channel and angle stiffeners are rigid in their attachment to the prestressed concrete Containment Structure and the liner.
b. As a compressed panel under biaxial compression, assuming the panel to be a portion of a large cylinder with a flexible stiffener system.

Figure 5-1 illustrates the actual physical configuration of the stiffening system for the liner plate. The channels function as horizontal stiffeners and the angles as vertical stiffeners.

For the solution, an initial deflected form for the liner plate is expressed in terms of a Fourier Series of the form:

$$\Delta = \sum_{n=0}^{\infty} \sum_{m=i}^{\infty} \Delta_{mn} \bullet \cos m\phi \bullet \sin \frac{n\pi x}{\lambda}$$

where: ϕ defines the central angle in a plan view of the cylinder from a point on the circumference where there is zero radial deflection to the point on the circumference where there is maximum radial deflection; x defines the radial deflection and λ defines the unsupported length in the vertical direction.

The stability analysis based on the above assumptions indicates that the critical buckling stress of the liner will be approximately 29,000 psi.

Under normal operating conditions, the maximum compressive stress in the liner will be approximately 23,000 psi. This reflects a buckling margin of 20%. Under LOCA conditions the expected stress in the liner plate will be 35,000 psi. Under this stress the overall structural stability of the liner plate can be maintained.

Also of concern is the nature of the state of stress and its behavior at the point of attachment between the stiffeners and the liner plate. Special tests have been conducted on simulated models of the liner plate and vertical stiffener assembly to determine the shear capacity of the angle and vertical stiffener assembly in order to determine the shear capacity of the angle anchorage. In the tests, two different configurations of support were used for the simulated continuous anchor. One case simulates the expected condition that will exist in the Containment Structure. A second case simulates the condition that might exist at an isolated location if the concrete were not in continuous contact with the anchor. Being guided in the proportioning of the liner plate stiffeners by the more critical values of shear transfer for the case of non-continuous contact will, in general, result in a margin of safety for progressive failure of anchors of approximately 2.7. The weld configuration shown in Figure 5-1 is felt to be adequate to transfer all loads that are considered in the design of the structure between the liner plate and the stiffener-anchors.

The conservative design approach of the stiffening system used in the liner plate to prevent significant distortions at accident conditions, and the stringent welding and weld inspection requirements ensure that the leak tightness of the liner plate at the LOCA condition will not change from that at the test condition.

In isolated areas the liner plate may have initial inward curvature due to construction. The anchors are designed to resist the forces and moments induced when a section of the liner plate between anchors has initial inward curvature.

The liner plate is anchored at all discontinuities to eliminate excessive strains. The forces in the liner plate at the discontinuities were evaluated and the anchors designed to resist these forces.

The liner adjacent to the penetrations is backed up by concrete. Refer to Figure 5-2 for a description of the anchoring arrangement at discontinuities and typical details.

The containment penetrations behave, partly or fully depending on their size, as elements of a pressure vessel. The sizes range from the small closure pieces for small pipe penetrations to larger components such as air locks and the equipment hatch. Those portions that are not backed up by concrete (the penetrations themselves) are treated as a pressure vessel and comply with ASME, B&PV Code, Section III, Nuclear Vessels, Subsection B, and are designed in accordance with the requirements of Section VIII, Paragraphs UG-27 through UG-33 for the service conditions outlined in Section 5.1.

The pressure part to thickened liner plate transition areas are designed and reinforced in accordance with the requirements of Paragraphs UG-36 through UG-41 as a welded assembly conforming to ASME, B&PV Code, Section VIII, Paragraph UW-13.

The air locks to thickened liner attachment rings were analyzed by finite-element methods; the membrane meridional, membrane hoop and the average radial stresses were investigated and the adequacy of design was verified.

The liner plate is considered as a composite part of the containment shell and as such, it is investigated by utilizing the strain and deformation data obtained by the finite-element analysis of the containment shell as tabulated in Table 5-1. See Appendix 5E for later tables associated with an evaluation to reduce the original amount of required containment prestress. The ASME B&PV Code is used only as a guideline to establish allowable strain limits, and not to verify the structural and leaktight adequacy of the liner.

In general, where the liner is firmly anchored and bonded to the concrete and maintains a strain compatibility with the concrete shell, the thickening of the liner will neither reduce nor increase the stresses. However at the openings, and particularly in the transition boundaries where the pressure elements of the penetrations are welded to the liner, the increase in the thickness of the steel plate will:

a. reduce the possible local stress concentrations, both in the steel plate and the adjacent concrete;
b. increase the stiffness of the plate and hence its buckling limit; and
c. increase the leaktight integrity of the transition welds.

At all penetrations the liner plate is thickened to reduce stress concentrations in accordance with the ASME, B&PV Code 1968, Section III, Nuclear Vessels. The thickened portion of the liner plate is anchored to the concrete by use of anchor studs all around the penetrations. For details of the penetrations see Figure 5-9. The sleeves, pipe cap and all welds associated with the penetrations are designed to resist all loads previously mentioned and also the prestress forces and internal design pressure.

At each location where a load is to be delivered to the walls, slab, or dome of the Containment Structure, an insert plate is provided to transmit the load through the liner. The insert plate is thickened and stiffened as required to deliver the load and to reduce stress concentrations in the liner. The insert plate is anchored to the concrete by appropriate anchors and shear connections. Typical examples of such insert plates are the polar crane brackets, and the floor beam brackets at the operating deck; typical details are shown in Figure 5-1.

5.1.4.4 Penetrations

All penetrations are pressure resistant, leak-tight, welded assemblies designed, fabricated, and tested in accordance with the ASME, B&PV Code, Section III, Nuclear Vessel Code.

Types of Penetrations

a. Electrical Penetrations

   Two types of electrical penetration assemblies are used - canister and unitized header. All electrical penetration assemblies are fabricated and tested in accordance with the ASME, B&PV Code, Section III, Nuclear Vessel Code. The canister type is inserted in a nozzle of suitable diameter integral with the Containment Structure and field welded on the inside end. The unitized header type is welded to the nozzle on the outside end. All penetration assemblies are provided with a means to pressurize for

monitoring of leakage. Any abnormal depressurization of an assembly is annunciated locally and in the Control Room.

There are three different types of electrical penetrations, used as follows:

1. Type 1 - 15 kV medium voltage power penetration canisters. These are 30" diameter cylinders constructed from steel plate (SA516, GR 70, 0.652" thick). Stainless steel header plates are then welded into each end containing epoxy bushings welded into the header plates.
2. Type 2 - Low voltage power and control penetration:
   a. Canister design: These are constructed of 10" diameter schedule 40 seamless steel pipe (SA 106B). Conductors are sealed with glass hermetics either direct fired into header plates or as assemblies welded into header plates.
   b. Unitized Header Design: Header is constructed of stainless steel, Type 304 (SA 240). Feedthroughs consist of conductors with resilient seal, are mounted and sealed to a header.
3. Type 3 - Instrumentation, thermocouple and coaxial penetrations:
   a. Canister design: See type 2.a above.
   b. Unitized Header design: See type 2.b above.

Figure 5-2 shows the different types of electrical penetration assemblies.

b. Piping Penetrations

Single barrier piping penetrations are provided for all piping passing through the containment walls. The closure of the pipe to the liner plate is accomplished with a pipe cap welded to the pipe and to the liner plate reinforcement. In the case of piping carrying hot fluid, the pipe is insulated and cooling is provided to reduce the concrete temperature to 150°F. Figure 5-2 shows typical hot and cold pipe penetrations. The modes of containment isolation are covered in Section 5.2.

The anchorage of penetration closure connecting pipes to the containment wall were designed as Seismic Category I structures to resist all forces and moments caused by a postulated pipe rupture. The design conditions include the maximum pipe reactions and pipe rupture forces.

The following design basis for typical piping penetrations was used to ensure the integrity of the liner penetration junction at the piping.

1. The penetration assembly, consisting of pipe cap and the assembly welds and welds to the liner plate, utilizes full penetration welds. The assembly is anchored into the wall concrete and designed to accommodate all forces and moments due to pipe rupture and thermal expansion.
2. The design basis is that the pipe penetration is the strongest point in the system when a pipe break is postulated. Pipe stops, increased pipe thickness or other means are used to attain this. Part of this basis also is that the operation of closure valves will not be impaired by any postulated pipe break.

c. Large Penetrations (Equipment and Personnel Access Hatches)

An equipment hatch opening, 19' in diameter, is provided as shown on Figure 5-3. The equipment hatch opening is covered on the inside of the Containment by a dished hatch, fabricated from welded steel, furnished with a double gasketed flange and bolted in place. The equipment hatch opening also has an outage use door at the exterior opening. The containment outage door is comprised of three assemblies: (1) a transition ring assembly welded directly to the equipment hatch nozzle steel liner plate; (2) a door frame assembly attached to the transition ring by means of bolts and locating pins that support all dead weight and seismic loads; and (3) a hinged door assembly. The frame of the containment outage door is equipped with fittings or penetrations that will allow electricity, compressed air, water, etc., to be run through the equipment hatch opening without going through the door. Flanges, cable penetrations, and isolation valves at these penetrations will be designed to withstand containment pressure resulting from postulated boiling in the RCS, as might occur during a loss of shutdown cooling. The design load to pass through the containment outage door is a reactor coolant pump motor on its transport trailer. For larger equipment, like replacement steam generator components, the bolted-on door frame assembly and door assembly may be removed from the transition ring assembly to restore the equipment hatch opening to its full diameter. Internal lugs welded to the nozzle liner plate and designed to carry the reactions due to the axial pressure loads and seismic loads to the nozzle liner plate may be removed and replaced when the door is restored.

Two personnel locks are provided. One of these is for emergency access only. Each personnel lock is a double door, welded-steel assembly. A quick-acting equalizing valve connects the personnel lock with the interior and exterior of the Containment Structure for the purposes of equalizing pressure in the two systems when entering or leaving. Typical details of the personnel access lock are shown in Figure 5-3.

The two doors in each personnel lock are interlocked to prevent both from being opened simultaneously and to ensure that one door is completely closed before the opposite door can be opened. Remote indicating lights and annunciators situated in the Control Room indicate the operational status of the door. Provision is made to permit bypassing the door interlocking system to allow doors to be left open during plant cold shutdown. An emergency lighting and communication system operating from an external emergency supply is provided in the lock interior.

d. Special Penetrations

1. Refueling Tube Penetration

A refueling tube penetration is provided for fuel movement between the refueling pool in the Containment Structure and the spent fuel pool in the Auxiliary Building. The penetration consists of a 36" stainless steel pipe installed inside a 42" pipe sleeve. The inner pipe acts as the refueling tube and is fitted with a gate valve in the spent fuel pool and an encapsulating pipe sleeve which is welded to the refueling pool liner and sealed off from the containment with a testable double O-ring blind flange in the refueling pool. This arrangement prevents leakage through the refueling tube in the event of a LOCA. The 42" pipe sleeve is welded to the containment liner.

Bellows expansion joints are provided on the transfer tube to compensate for any differential movement between the tube and the building structures. Figure 9-14 is a drawing of the refueling tube installation. The design basis for each expansion joint is listed below:

AUX. BUILDING FUEL POOL EXPANSION JOINT	CONTAINMENT REFUELING POOL EXPANSION JOINT
External design pressure 28 psig	External design pressure 29 psig
Internal design pressure 28 psig	Internal design pressure 29 psig
Design temperature 150°F	Design temperature 273°F
Lateral movement 1-1/2"	Lateral movement 1/2"
Axial movement 1-1/2" (expansion or contraction)	

Displacements were selected to accommodate the maximum differential building settlements. The expansion joint in the refueling pool may be visually inspected from the outside with a periscope when the refueling pool is empty. Repair would probably involve removing the 54" OD pipe that forms the containment boundary. The outside of the expansion joint in the spent fuel pool may be visually inspected by draining the pool or by remote means. A test connection on the bellows provides a means of testing bellows integrity. Repair would require draining the spent fuel pool.

2. Containment Supply and Exhaust Purge Penetrations

   The ventilation system purge penetrations are equipped with a testable double O-ring blind flange in the penetration room and a tight-seating butterfly valve inside containment used for isolation purposes. The blind flange is used to provide containment integrity during Modes 1-4. The valve is manually opened for containment purging in Modes 5 and 6 as described in Section 9.8.2.2.

3. Containment Vent Penetration

   This system is equipped with two valves to be used for isolation purposes. These valves are opened by a handswitch in the Control Room to vent containment pressure during power operation. Although control of hydrogen in Containment following an accident is not required, this penetration may be used as a hydrogen purge.

Design of Penetrations

a. Design Basis

   Penetrations conform to the applicable sections of American Standards Association (ASA) N6.2-1965, "Safety Standard for the Design, Fabrication, and Maintenance of Steel Containment Structures for Stationary Nuclear Power Reactors" which has since been withdrawn. All personnel locks and any portion of the equipment access door extending beyond the concrete shell conform in all respects to the requirements of ASME, B&PV Code, Section III, Code for Nuclear Vessels. All future penetrations will conform to ASME, B&PV Code, Section III, Division 1 for fluted head analysis, and Division 2 for those integrated with steel in concrete openings.

Each line which penetrates the containment and contains high-pressure or high-temperature fluids (steam, feedwater, and steam generator blowdown) passes through a structural steel sleeve mounted on the containment wall. This sleeve acts as a positive stop to prevent whipping associated with fracture of a line containing high internal energy and thereby prevents damage to the penetration and breaching of the containment.

Further protection of each line, necessary to preclude pipe rupture between the penetration and the first valve, is accomplished by shortening the exposed length of pipe and installing the first valve as close as possible to the internal or external wall of the structure, dependent upon valve operating and maintenance clearances. Design bases which apply to the provision of automatic and manual isolation valves in the penetration lines are contained in Section 5.2.

All penetrations, except the equipment hatch and emergency personnel lock, are inside the Auxiliary Building; therefore, the temperature of Auxiliary Building penetration material will not fall below 30°F. Using the assumption of +60°F temperature inside the containment and outside air temperature of +20°F, the temperature of the equipment hatch and emergency personnel door will not be below +30°F, during startup, operation, or cooldown of the reactor. An investigation was made to determine necessity and/or feasibility of protecting the exterior surface of these penetrations. None was required. Two temperature indicators are provided to monitor the temperature inside the containment. A technical specification is not considered to be necessary for the above reasons.

b. High-Temperature Penetrations

The main high-temperature piping consists of two penetrations for feedwater, two penetrations for main steam, two penetrations for steam generator blowdown, one for the reactor coolant letdown line, and one for the reactor coolant sampling line. These have a maximum operating temperature range between 435°F and 653°F. Thermal insulation is provided on the outside diameter of each line and separate coolant circulation, with instrumentation suitable for flow monitoring, is provided in the air gap between the insulation and the penetration liner sleeve. The combination of insulation and coolant circulation is designed to restrict the maximum temperature in the concrete to 150°F.

For the condition of loss of penetration coolant circulation, the maximum steady state temperature in the concrete will be 300°F at the penetration surface and decreases to 120°F at a maximum radial depth of 48" in the containment wall. Actual peak temperatures in the penetrations resulting from LOCA conditions are expected to subside within six hours. A maximum temperature of 390°F may be tolerated for 120 days (Reference 5) without appreciable loss of concrete strength.

The basis for limiting strains in the penetration steel is the ASME, B&PV Code, Section III, Nuclear Vessels, Article 4, 1965, and therefore, the penetration structural and leak-tightness integrity will be maintained. Local heating of the concrete immediately around the penetration will develop compressive stress in the concrete adjacent to the penetration and a negligible amount of tensile stress over a large area. The mild steel

reinforcing added around penetrations will distribute local compressive stresses for overall structural integrity.

c. Penetration Materials

The material for the penetrations, including the personnel and equipment access hatches together with the mechanical and electrical penetrations, is carbon steel and conforms with the requirements of the ASME, B&PV Code, Nuclear Vessel Code. As required by the Nuclear Vessel Code, the penetration materials which form the pressure boundary meet the necessary Charpy V-notch impact values at a temperature 30°F below the lowest service temperature.

1. Piping Penetration Materials

Materials specifications are listed below:

Piping Penetration Material	Specification
Penetration Sleeve	ASTM A155
Penetration Reinforcing Rings	ASTM A516
Penetration Sleeve Reinforcing	ASTM A516
Bar Anchoring Rings and Plates	ASTM A516
Rolled Shapes (nonpressure boundaries)	ASTM A36

2. Electrical Penetration Materials

The penetration sleeves to accommodate the electrical penetration assemblies are Schedule 40 carbon steel pipe, except where otherwise noted.

3. Access Penetration Materials

The equipment hatch and personnel access locks materials are all ASTM A516 made to ASTM A300.

Installation of Penetrations

The qualification of welding procedures and welders is in accordance with Section IX, "Welding Qualifications" of the ASME, B&PV Code. The repair of defective welds is in accordance with paragraph N-528 of Section III, "Nuclear Vessels" and Section VIII of the Code.

Testability of Penetrations

Only the following penetrations are ASME, B&PV Code, Section III, Class B penetrations as classified in the Atomic Energy Commission (AEC) Technical Safety Guide, "Reactor Containment Leakage Testing and Surveillance Requirements," December 15, 1966. As Class B penetrations, they are subject to individual periodic leak-rate tests separate from the integrated Class A tests.

a. Equipment Hatch
b. Personnel Lock
c. Emergency Personnel Escape Lock
d. Refueling Tube
e. Purge Line Inlet and Outlet

5.1.5 INTERIOR STRUCTURE

For the original compartment designs, the occurrence of a LOCA was postulated to result from the rupture of the RCS piping, including the main loop piping, either within the reactor cavity or the SG compartments of the containment. For the current compartment designs, breaks are not postulated to occur in the main loop piping based on the Leak-Before-Break Evaluation (References 6 and 7). The design of the Babcock & Wilcox, Canada replacement steam generators also incorporates the application of leak-before-break, which included dynamic analysis of steam generator internals (U-tubes, divider plate, lattice grids, and shroud) for the effects of the most limiting postulated break (12" pressurizer surge line break). American Society of Mechanical Engineers Code-reconciled design and methods were used to install the replacement steam generators to ensure the equivalency of the replacement steam generators-to-RCS piping connections to the original steam generator–to-RCS piping connections, and thus the continued validity of the assumptions made in References 6 and 7. Since only main loop piping is present in the reactor cavity, no LOCA is currently postulated to occur in this compartment. However, smaller bore piping connected to the RCS is present in both steam generator compartments and the pressurizer compartment. The following discussion regarding a LOCA in the reactor compartment is provided as historical design information only.

5.1.5.1 Design Basis

Design of the containment interior structures evolves around four basic systems: The primary coolant system, the turbine steam system, the engineered safety system, and the fuel handling system.

The structures which house or support the basic systems are designed to sustain the factored loads of Appendix 5A.

The design bases applied are:

a. The structures will sustain all operating dead and live loads, thermal loads, and design seismic loads, without exceeding code allowable stresses.
b. Loads and deformations resulting from a LOCA failure and its associated effects in any one of the basic systems will be sustained and restricted such that propagation of the failure to any other system is prohibited. In addition, a failure in one loop of the Nuclear Steam Supply System will be restricted such that propagation of the failure to the other loop is prohibited.

Loss-of-coolant accident loads and associated effects include:

a. Thrust loads resulting from rapid mass release from a pipe break in any system;
b. Pressure buildup in locally confined areas such as the reactor cavity or the secondary shielding compartments; and
c. Jet forces resulting from the impingement of the escaping mass upon adjacent structures. The following method was employed to compute the jet forces:
    1. Rupture may occur anywhere on portions of the main coolant pipes that are near to the structure or component under investigation. The jet force due to a double-ended break acts along the pipe axis, which may change its direction. The jet force due to a slot break may act in any radial direction normal to the pipe axis.

2. Both the double-ended and the slot break expose an area equal to the inside cross-sectional area of the pipe ruptured. The length of a slot break is equal to twice the diameter of the ruptured pipe.
3. The magnitude of the jet force is computed by the following equation, and does not change with distance to target:

   F = 2.0 x Operating Pressure x Inside Cross-Sectional Area of Pipe
4. The area of the jet plume diverges at a half angle of 10° from the pipe opening. The jet force is evenly distributed to the area of plume at any distance to obtain the impinging pressure on the structure.
5. A spectrum of all possible breaks are considered for a particular structure, and the ones that produce maximum stresses in the structure are used for design.

d. Erosion effects of jet spray.
e. Pipe whipping following a break in the pipe.
f. Rapid rise in ambient temperature to 276°F and accompanying rise in ambient pressure to 50 psig. All Containment Structures have been evaluated for the revised maximum vapor temperature referenced in Section 14.20.
g. Missiles as described in Section 5.1.5.3.

The containment interior structures were analyzed by utilizing a lumped parameter model which treated the exterior shell, base slab, foundation media and the interior structures as a coupled system, and included details of the interior structures. The ground response spectra, as shown in Section 2.6.3, were used to determine the shears, moments, forces and displacements in the various structural, components, expected to be induced by the SSE and OBEs. The method employed is basically the analysis through the response of the normal modes to spectral accelerations, and is outlined in Section 5.1.3.2 as part of the "Containment Structure Design Analysis." Seismic induced shears, moments and forces are then multiplied with the load factors for Seismic Category I structures as indicated in Section 5A.3.1. When checking each component, particular attention has been paid to tall and slender, or tall and cantilevered portions for possible further amplification. Such components were investigated by utilizing the floor response spectra.

Seismic analysis for the interior structures was done using procedures outlined in Section 5.1.3.2.

Where concrete structures such as the primary shield wall are subjected to sustained internal heat buildup, mechanical cooling devices are included to keep the internal temperatures below 150°F. Localized concrete temperatures up to 200°F are acceptable.

The total heat generation rate in the primary shield includes contributions from the following radiation sources: fission neutrons and gammas; core secondary gammas; secondary gammas from the core shroud, core support barrel, the reactor vessel, and the intermediate water regions; and secondary gammas in the concrete primary shield. Secondary gamma sources due to neutron scattering and capture were based on neutron distributions calculated using methods described in Chapter 3. The computer program QAD-P5 incorporates a point-kernel numerical integration method for the gamma radiation and a point-kernel moments method for each of the source contributions listed above and the heating rates due to the several contributions summed. The temperature gradient of the primary shield wall resulting from radiation-generated heat is combined with the

temperature gradient resulting from convective heat from the reactor to form a combined temperature gradient in the primary shield wall. The combined gradient was used in the thermal stress analysis and the resulting stresses in the wall were determined by using the design methods established by ACI 505-54. These stresses were combined with the stresses resulting from the analysis of loading combinations as described in Section 5.1.5.1. The critical stresses were then used to evaluate required reinforcing in both directions. All stresses are within the allowable as established Appendix 5A.

5.1.5.2 Design Loads and Materials

a. Design Loads:

The reactor cavity wall, the steam generator compartment walls, and containment interior structures are all Seismic Category I structures, the final design of which satisfied the most severe of the load combination equations of Appendix 5A.

b. Materials:

The following materials have been used in the construction of the Containment Structure interior:

Concrete	f_c'= 5000 psi @ 28 days
Rebar	A615, Gr 60
Plate Steel	A441 & A533
Structural Steel	A36 & A441
Anchor Bolts	A325, A354 & A490

5.1.5.3 Missile Protection Inside Containment

High pressure RCS components which could be a source of missiles are suitably screened, either by the concrete shield wall enclosing the reactor coolant loops, by the concrete operating floor or by special missile shields, to block any passage of missiles to the containment walls. Potential missile sources are oriented so that the missile will be intercepted by the shields and structures provided. A shield is provided over the control rod drive mechanism to block any missiles generated from postulated fracture of the nozzles.

All internally-generated missiles inside the Containment Structure are listed in Table 5-2. For all other internally-generated missiles outside the Containment Structure, see Section 5.3.1.1. All Seismic Category I structures or parts of structures have been checked for impact of missiles. The modified Petry formula was used for checking the effects of missiles on the structure at the point of impact. Even under extreme assumptions, missiles do not penetrate the concrete barriers completely.

Missile protection inside the Containment Structure is provided to comply with the following criteria:

a. The Containment Structure and liner are protected from loss-of-function due to damage by such missiles as might be generated in a LOCA for break sizes up to and including the double-ended severance of a reactor coolant pipe.
b. The engineered safety features and components required to maintain containment integrity are protected against loss-of-function due to damage by such missiles.

Missile protection necessary to meet the above requirements was implemented using the following methods:

a. Components of the RCS were examined to identify and to classify missiles according to size, shape, and kinetic energy for purpose of analyzing their effects.
b. Missile velocities were calculated considering both fluid and mechanical driving forces which can act during missile generation.
c. The RCS is surrounded by reinforced concrete and steel structures designed to withstand the forces associated with the double-ended rupture of a reactor coolant pipe and designed to stop missiles.
d. The structural design of the missile shielding takes into account impact loads and is based upon the state of the art of missile penetration calculational techniques.

The types of missiles for which protection is provided are:

a. Valve stems;
b. Valve bonnets;
c. Instrument thimbles; and
d. Various types and sizes of nuts and bolts.

Protection is not provided for certain types of missiles for which postulated accidents are considered incredible because of the material characteristics, inspections, quality control during fabrication, and conservative design as applied to the particular component. Included in this category are missiles caused by massive, rapid failure of the reactor vessel, steam generator, pressurizer, and main coolant pump flywheels and casings.

It is not expected that the polar crane will become or generate an internal missile. The crane is anchored with seismic lugs and the crane and its components are designed for the OBE and SSE. Additionally, design features and administrative controls are in place to minimize the probability of a load drop from the polar crane. A description of our means of controlling heavy loads is presented in Section 5.7.

5.1.5.4 Thermal Gradients

Ventilation and cooling systems maintain thermal gradients at a level low enough to have very small structural effects on the concrete walls. These effects are, nevertheless, considered in the design.

Reactor Cavity Wall

Energy is deposited in the concrete of the reactor cavity wall by nuclear radiation emanating from the surface of the reactor vessel. In the equilibrium condition, assuming no axial leakage, all the deposited energy is removed either by the air-cooling system at the inner surface of the cavity wall or by convection from the outer surface. In order to find the temperature distribution within the concrete, an analytical expression for the energy deposition distribution is first derived. This expression is substituted in the heat diffusion equation which is solved for temperature using the temperature boundary conditions at the inner and outer face of the concrete.

Steam Generator Compartments

The ventilation system provided eliminates temperature gradients across the secondary shield walls, across the refueling pool walls and across the operating floor.

5.1.5.5 Differential Pressures

Generally, the occurrence of a LOCA is postulated to result from a rupture of the primary system piping either within the reactor cavity or the steam generator compartments of the containment. A pipe rupture of this type, within a compartment, results in the expulsion of high enthalpy water that flows out of the ruptured pipe, flashing partly to steam. As the pressure builds up within the compartment, the steam-air-water mixture flows through openings into the main containment. The maximum pressure differential will depend on the number and shape of the openings leading between the compartments, the volume of each compartment, and the blowdown rate from the broken pipe.

Differential pressure analyses are made with the Bechtel computer program COPRA, which calculates the transient pressure responses of two containment compartments during a LOCA. COPRA calculates a mass and energy balance of the two-phase, two-component steam-water-air mixture as primary coolant enters the compartment during the LOCA and exits through vents and openings into the main containment building. There is no provision in the code for heat transfer to structures or for engineered safety features. These options generally have a negligible effect on compartment pressures for the short time following the rupture within which peak differential pressures occur.

Because of this short time interval between the LOCA and the peak compartment pressure differential, each case analyzed is divided into very small time intervals, generally equal to or less than 0.1 msec. The thermodynamic equations are solved for each time advancement.

The steam, water and air throughout each compartment are in thermal equilibrium at all times. Water, steam, and air entering a compartment are mixed homogeneously and instantaneously; no accumulation of water occurs on the walls or in the sump.

A COPRA Summary Document which lists and discusses the program assumptions, is contained in Reference 9. This document is on file with the Nuclear Regulatory Commission (NRC).

The discussion of the results of the analyses performed for each interior containment compartment is contained in FSAR [Final Safety Analysis Report] Section 14.16.5, as revised by FSAR Amendment No. 29, Revision 18 (currently Updated Final Safety Analysis Report Section 14.20).

The compartment walls have been designed for jet impingement forces and differential pressures, both assumed to occur simultaneously with the SSE.

This design has the following conservative considerations:

a. A dynamic load factor of two is applied to the maximum jet load. (The jet load is based on sudden severance of the primary loop piping nearest to the wall.)
b. The differential pressure and jet impingements are considered to be in phase.

As dictated by design, any transient response of the containment compartment walls is expected to contain the most severe accident postulated.

Reactor Cavity

There are two types of openings for flow out of the reactor cavity into the main containment volume:

a. Openings around the main coolant pipes - 40.0 ft^2
b. Openings around the reactor vessel seal ledge - 173 ft^2

The current plant design includes a permanent refueling pool seal that further restricts the opening around the reactor vessel. This analysis is provided as historical design information only (Reference 7).

The areas around the main coolant pipes extend along the annular space between the pipes and the walls of the pipe tunnels. A calculated nozzle flow coefficient of 0.61, based on the geometry of these flow spaces, is utilized. The opening around the refueling seal ledge is treated as an orifice. Flow coefficients for orifice geometries are supplied automatically by the COPRA computer code.

Immediately after a pipe rupture, the volume available to the expanding steam within the reactor cavity is the free volume below the seal ledge.

Both guillotine and slot primary pipe failures have been considered:

a. For the guillotine break, the coolant pipes are partially restrained by the tunnel walls. Restraining the primary pipes in this manner gives a flow area of 0.61 ft^2 for failure of the 42" line, which results in a cavity peak differential pressure of 23 psi.
b. The slot longitudinal break has a length of twice the inside pipe diameter and an area equal to the pipe cross-sectional area. The flow from the part of the break within the pipe tunnel is divided between the reactor cavity and the steam generator compartment, while the flow from the part of the break that is between the primary shield wall and the nozzle of the vessel enters the reactor cavity only. The total flow of mass and energy into the reactor cavity is approximately 27% of the flow from a 42" single-ended rupture. As the reactor cavity pressure builds up, the flow leaving the pipe within the pipe tunnel will enter the steam generator compartment; however, credit for this effect is conservatively ignored to simplify the problem. The peak differential pressure resulting from the slot failure is 31 psi.

The following table summarizes the input parameters used for the computer analysis of reactor cavity pressurization:

Main containment free volume	2.0x106 ft^3
Reactor cavity free volume	$5.135x10^3$ ft^3
Nozzle-type relief area (around piping)	40.0 ft^2
Nozzle coefficient	0.61
Orifice-type relief area (around seal ledge)	173.0 ft^2
Initial containment temperature	110°F
Initial containment pressure	14.7 psia
Initial containment humidity	50%

Note that this analysis was redone for the neutron shield with no significant differences.

Steam Generator Compartments

For the steam generator compartments, only the double-ended guillotine break in the hot leg is considered since it provides the largest rate of energy and mass release. The relief areas are divided into three classes: long, sharp-edged nozzles, sharp-edged orifices and well-rounded orifices. An orifice coefficient of 0.61 is applied to the long nozzles and a coefficient of 0.97 is applied to the well-rounded orifices; coefficients for sharp-edged orifices are supplied by the computer. The compartment volumes and total flow areas are listed below:

Compartment	Volume	Long Sharp -edged Nozzles	Sharp -edged Openings	Well Rounded Openings	P
East	[(a)]53,980 ft^3	356 ft^2	770 ft^2	1,072 ft^2	16.4 psi
West	51,500 ft^3	182 ft^2	414 ft^2	1,072 ft^2	18.4 psi

(a) East volume is greater than west because east includes pressurizer as well as one steam generator and two reactor coolant pumps.

The initial conditions and the main compartment volume are the same as those used in the reactor cavity.

5.1.5.6 Design Bases Temperature and Pressure Differentials

Safety factors were not determined or established for pressure and temperature acting alone. The design and analysis methods as applied to the interior structures, accounted for and investigated the effects of temperature and pressure in conjunction with the other loads occurring in those conditions as stated in Appendix 5A. The associated individual safety margins can best be examined by: discussing the contribution of these loads to the total stress intensities, or to the total ultimate load carrying capacity of the structure or component under the two main categories of design loading conditions.

The two main design loadings conditions and the serviceability required of the interior structures in each case are that:

a. They provide support during plant operation and prevent the occurrence of a LOCA from:
    1. Normal operating loads (including dead loads)
    2. Design live loads
    3. Hydrostatic loads
    4. Thermal loads
    5. OBE seismic loads

b. They mitigate its consequences, should a LOCA occur, by protecting the containment and all engineered safety features systems from:
    1. Blowdown forces (including jet thrust and impingement loads)
    2. Whipping pipes
    3. Missiles
    4. Differential pressures

5. SSE seismic loads
6. Loads a.1, and others, if applicable

The safety factor of the structure is the ratio of allowable stresses to the computed stresses in case (a) above, and the ratio of the ultimate load resisting capacity of the structure to the total applied loads in case (b).

In general, this ratio is not the same for all components of the interior structure and varies with both the modes of stress or loading and the hazard associated with the structure or component thereof (i.e., some of the components that were governed by radiological shielding requirements have capacities much higher than the design loads; uniaxial, flexural normal, shearing torsional, tensile and compressive stresses were treated differently). Further, the loads above were combined per Appendix 5A load combination equations which have an inherent factor of safety defined by their load coefficients. No credit is taken for this safety factor.

For the operating loads, the minimum safety margin is as determined from ACI 318-63 code for reinforced concrete, and AISC Specification, 1963, for structural steel. The contribution of the operating temperatures is negligible in all components except the reactor cavity wall, for which additional reinforcing steel was furnished for the thermal stresses in accordance with the requirements of ACI 505-59. The accident condition controlled the design of most of the interior structures, including the reactor cavity wall, the secondary shield walls which house the RCS, and all major vessel support structures. Where stresses due to blowdown forces were in the same direction and thus combined with the stresses due to other loads including temperature and pressure, the share of the former ranged from 60 to 80%, thus resulting in an increase of 2.5 to 5 times the inherent safety factor for the latter loads acting alone. Where temperature and pressure stresses acted alone, the safety factors inherent in the load combination equations were increased by 3.0 and 1.5 in the operating and accident cases respectively, for both reinforcing and structural steel. In all cases, the safety margin for concrete stresses were kept higher than steel in order to preclude brittle modes of failure.

The calculated differential pressures and temperature gradients, and those that have been used as the design bases of the major interior structures are listed below:

	ΔP (Design)	ΔP (Calculated)	ΔT (Design)	ΔT (Calculated)
East Steam Generator Compartment Walls	28 psi	16.4 psi	None	None
West Steam Generator Compartment Walls	28 psi	18.4 psi	None	None
Reactor Cavity Wall	96 psi	31.0 psi[(a)]	30°F/7'	6.7°F/7'

[(a)] The current plant design includes a permanent refueling pool seal which further restricts the opening around the reactor vessel. This analysis result is provided as historical design information only (Reference 7).

5.1.6 LIGHTNING PROTECTION OF CONTAINMENT

Lightning protection is provided over the dome of the containment vessel and consists of the following:

One 1/2"x24" copper air terminal is placed in the center of the dome. Eight equally spaced 1/2"x25" air terminals are installed on a 20'-diameter circumference. These are connected to closed loop of 2/0 AWG cable. Four cables of like size connect the loop with the center air terminal. Another 16 equally spaced 1/2"x24" air terminals are installed on 40' circumference. These are connected to a closed loop of 2/0 AWG cable. Another 20 equally spaced 1/2"x24" air terminals are installed on a 69'3" radius circumference.

These are connected to a closed loop of 2/0 AWG cable. Four equally spaced 1/2"x24" air terminals connect the three loops. Four 2/0 AWG down conductors connect the outer loop to the ground grid. Ground guards are provided to protect down conductors to an approximate height of 8' above grade.

5.1.7 CATHODIC PROTECTION

The containment cathodic protection system and related environmental or galvanic corrosion protection schemes are explained in the following discussion.

Heavy waterproofing (40 mils thickness) membrane is used underneath the containment base slab, within the 4"-thick mud mat and around the cylindrical shell up to finish grade. This membrane is protected to full height by 1/2" (minimum) thick asphalt-impregnated fiber board prior to backfilling. Remotely-located shallow anodes are used in cathodic protection system. Anodes placed approximately 100' from the membrane could protect the structure regardless of the total cross-section of apertures and would provide protection as required for pipes and tank bottoms. Zinc and/or copper sulphate permanent reference electrodes are located in the soil to enable measurement of protective gradients around the foundation. This scheme is based on the concept that the containment building foundation steel is formed with an inhibitive concrete cover, a heavy waterproofing membrane and a relatively low chloride/oxygen environment. Steel embedded in or covered by concrete in the containment sub-structure will be protected by the waterproof membrane. The system is conservatively designed for a 40-year life, derating manufacturer's recommendations for anodes by approximately 50%.

The surface of the exposed liner plate was protected by an initial cleaning by wire brushing or sandblasting, and then coated with Amercoat zinc paint or its equivalent at the fabrication plant. After erection, all exposed areas adjacent to field welds were cleaned or reprimed, and the entire exposed face was painted with a finish coat. The outside of the liner is protected by a minimum of 3-1/4' of prestressed concrete, which is cast against the liner offering a very high degree of corrosion protection.

The ACI Building Code Requirements for Reinforced Concrete (ACI 318-63), Section 808, Concrete Protection For Reinforcing, have proved to be effective for preventing chemical corrosion of concrete reinforcement. The reinforcing concrete protection exceeds Section 808 requirements by 50% or more. Tendon sheathing has a minimum of 11" of concrete cover at any location in the Containment Structure.

5.1.8 LEAKAGE MONITORING SYSTEM

No continuous leakage monitoring system is provided.

The barrier to leakage in the Containment Structure is the 1/4" steel liner plate. All penetrations were continuously welded to the liner plate before the concrete in which they are embedded was placed. These penetrations, shown on Figures 5-2

and 5-3, became an integral part of the liner and were so designed, installed, and tested.

The steel liner plate is securely attached to and is an integral part of, the prestressed concrete Containment Structure which is conservatively designed and rigorously analyzed for the extreme loading conditions of the postulated LOCA, as well as for all other types of anticipated loading conditions. Thorough controls were maintained over the quality of all materials and workmanship during all stages of fabrication and erection of the liner plate and penetrations, and during construction of the entire Containment Structure.

The comprehensive program for preoperational testing, inspection, and post-operational surveillance is described in detail in Section 5.5 and is summarized in the following paragraphs.

During construction, the entire length of every seam weld in the liner plate was leak tested. Individual penetration assemblies were shop tested. Welded connections between penetration assemblies and the liner plate were individually leak tested after installation. Following completion of construction, the entire Containment Structure, the liner and all its penetrations were tested at 115% of the design pressure to establish structural integrity. The initial leak rate test of the entire structure was conducted at 50 and 100% of the calculated peak pressure to demonstrate vapor tightness, and to establish a reference for periodic leak testing for the life of the plant.

Penetrations such as the permanent equipment hatch opening and personnel access locks cannot be opened except by deliberate action. The personnel access locks are interlocked and provided with alarm devices so that the Containment Structure cannot be breached unintentionally. The liner plate over the foundation slab is protected by cover concrete. Wherever access to the liner plate welds is not possible, means are provided so that they can be tested for leakage. The liner plate is protected against corrosion by suitable coatings and by cathodic protection. Walls and floors for biological and missile shielding also provide protection for the liner plate.

Once the adequacy of the liner plate was established initially, there is no reason during the life of the plant to anticipate progressive deterioration which would reduce the effectiveness of the liner as a vapor barrier. Inside the Containment Structure, the atmosphere is subject to a high degree of temperature control. The outside of the liner is protected by prestressed concrete which is resistant to all weather conditions.

Inspection on a periodic basis, as necessary, may be conducted in all accessible areas during full power operation. Biological shielding is provided to reduce direct radiation from the RCS to acceptable limits. A visual inspection of the Containment Structure, from the inside and outside, will be conducted during regularly scheduled unit shutdowns.

All penetrations, except the following, are located in groups, and a penetration room is located at each group.

a. Equipment Hatch Opening
b. Personnel Access Lock
c. Emergency Personnel Access Lock
d. Refueling Tube

e. Purge Line Inlet and Outlet
f. Containment Emergency Sump

Any leakage that might occur from these penetrations will be collected and exhausted through vents or drains. In this manner, leakage which might occur from these groups of penetrations will be isolated from leakage which might occur through the Containment Structure, itself.

Provisions are made such that these penetrations may be pressure tested for leakage during normal operation.

The containment normal sump penetration is another exception that is not located in a penetration room. However, there are no provisions made to collect and exhaust leakage from this penetration or to enable pressure testing during normal operation. This penetration is further described in Section 5.2.2.

Within the penetration rooms, provisions are made such that individual penetration assemblies with resilient seals may be pressure tested for leakage during normal operation. This degree of control over leakage through penetrations greatly reduces the probability of undetected leakage for the Containment Structure as a whole.

A considerable background of operating experience is being accumulated on containment and penetrations. Full advantage of this knowledge is taken in all phases of design, fabrication, installation, inspection, testing, and operation.

For the foregoing reasons, it has been concluded that a continuous leakage monitoring system is unnecessary. Since there is no such system provided, there can be no misoperation or malfunction, which in itself might constitute a hazard. The steel-lined Containment Structure is self-sufficient, and other than valves and hatch doors, there are no operating parts. The containment boundary is extended only by specific penetrations which are further described and tabulated in Section 5.2, "Isolation System."

5.1.9 REFERENCES

1. A.C. Eringen and A.K. Naghdi, "State of Stress in a Circular Cylindrical Shell with a Circular Hole"
2. Levy, Samuel, A.E. McPherson, and F.C. Smith, "Reinforcement of a Small Circular Hole in a Plane Sheet Under Tension," Journal of Applied Mechanics, June 1948
3. K.R. Wickman, A.G. Hopper, and J.L. Mershon, "Local Stress in Spherical and Cylindrical Shells due to External Loadings," Welding Research Council Bulletin No. 107, August 1965
4. HTGR and Laboratory Staff, Prestressed Concrete Reactor Vessel, Model 1, GA7097
5. Advanced HTGR Staff, Prestressed Concrete Reactor Vessel, Model 2, (GA7150)
6. CEN-367-A, “Leak Before Break Evaluation of Primary Coolant Piping in Combustion Engineering Designed NSSS,” February 1991
7. Letter from Mr. D. G. McDonald (NRC) to Mr. R. E. Denton (BGE), dated February 3, 1994, Installation of a Neutron Shield/Pool Seal at the Calvert Cliffs Nuclear Power Plant, Unit Nos. 1 and 2 (TAC Nos. M87176 and M87177)

8. Letter from NRC to Mr. E. C. Sterling, III, Chairman CEOG, dated October 30, 1990, Acceptance for Referencing Topical Report CEN-367, “Leak-Before-Break Evaluation of Primary Coolant Loop Piping in Combustion Engineering Designed Nuclear Steam Supply Systems”

9. Containment Pressure Analysis, NS731 TN, December 1968

10. Letter from C. H. Cruse (BGE) to Document Control Desk (NRC), dated April 2, 1999, First Annual Amendment to Application for License Renewal

TABLE 5-1

STRESS ANALYSIS RESULTS[8]

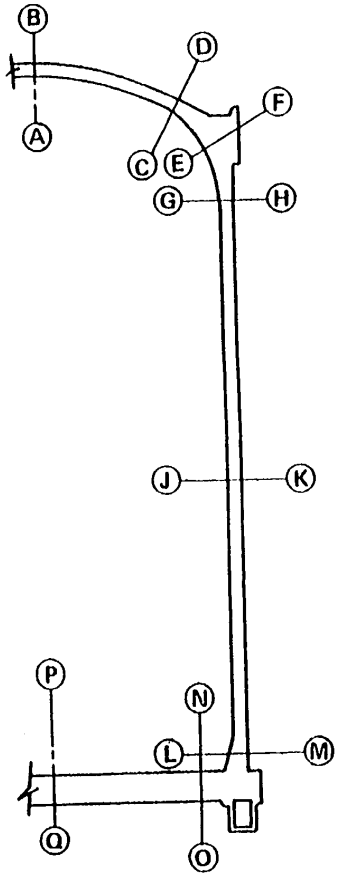

KEY ELEVATION
(Showing location of reference sections)

LOCATION	STRUCTURAL DATA			
	CONCRETE		REINFORCING STEEL	
	f'_c - psi	t - in	P_m - %	P_h - %
A	5000	39	.260	.094
B	5000	39	.619	.214
C	5000	55.6	.159	.150
D	5000	55.6	.253	.232
E	5000	138.12	.060	.060
F	5000	138.12	.286	.112
G	5000	45	.316	.185
H	5000	45	.741	.289
J	5000	45	.235	.235
K	5000	45	.235	.235
L	5000	70.2	.315	.247
M	5000	70.2	.570	.247
N	4000	120	.223	.185
O	4000	120	.447	.479
P	4000	120	.286	.222
Q	4000	120	1.144	.514

TABLE 5-1

STRESS ANALYSIS RESULTS[8]

ALLOWABLE STRESSES

WORKING STRESS DESIGN	YIELD STRESS DESIGN
SHELL CONCRETE:	
f_a = 1500 psi	$f_a = \phi_a (f_c) = (0.85)(5000) = 4{,}250$ psi
f_{ce} = 3000 psi	$f_{ce} = \phi_{ce} (f_c) = (0.90)(5000) = 4{,}500$ psi
BASE CONCRETE:	
f_{ce} = 1800 psi	$f_a = \phi_a (f_c) = (0.85)(4000) = 3400$ psi
	$f_{ce} = \phi_{ce} (f_c) = (0.90)(4000) = 3600$ psi
STEEL: A615, GR 60	
f_s = 30,000 psi	$f_s = \phi (f_y) = (0.90)(60{,}000) = 54{,}000$ psi

TABLE 5-1

STRESS ANALYSIS RESULTS[8]

D + F + L (Stresses in psi) Construction Case I

		MERIDIONAL			HOOP			SHEAR		
	SECTION	σ_e OUTSIDE	σ_e INSIDE	σ_a AXIAL	σ_e OUTSIDE	σ_e INSIDE	σ_a AXIAL	τ	V_{ci}	V_{cw}
Shell										
	A - B	-827	-1630	-1256	-814	-1609	-1207	-23	105	687
	C - D	+243	-1630	-609	+77	-734	-250	+32	45	452
	E - F	-248	-784	-464	+136	-863	-330	+15	43	360
	G - H	-1	-26	-618	-55	-1154	-613	-40	104	513
	J - K	-1	-8	-664	-575	-1645	-1120	-8	69	427
	L - M	2	-27	-499	-481	-645	-583	6	98	359
Base										
	N - O	113	-251	-41	565	-426	-29	32	138	157
	P - Q	560	-971	-69	565	-470	-12	44	135	123

TABLE 5-1

STRESS ANALYSIS RESULTS[8]

CONTAINMENT STRUCTURE - SUMMARY OF CONCRETE AND REINFORCING STEEL STRESSES (psi)

SECTION		LOAD CASE	CONCRETE COMPUTED σ_{em}	σ_{eh}	σ_{am}	σ_{ah}	τ	COMPUTED VS. ALLOWABLE $\frac{\sigma_e}{f_{ce}}$	$\frac{\sigma_a}{f_a}$	$\frac{\tau}{v}$
	II	D+F+L+1.15P	-997	-935	-591	-542	-6	0.332	0.394	0.017
	III	D+F+L+T_O+E	-2141	-2363	-1307	-1324	20	0.788	0.883	0.056
A-B	IV	D+F+L+T_A+P	-2990	-2985	-545	-510	7	0.993	0.363	0.020
	V	1.05D+F+1.5P+ T_A	-2610	-2213	-215	-61	2	0.580	0.051	0.003
	VI	1.05D+F+1.25P+ T_A+1.25E	-2048	-2205	-652	-519	24	0.490	0.153	0.040
	VII	D+F+P+ T_A+E'	-2247	-2392	-804	-732	17	0.532	0.189	0.030
	II	D+F+L+1.15P	-814	-573	-240	50	68	0.271	0.160	0.200
	III	D+F+L+T_O+E	-2210	-1367	-645	-293	65	0.737	0.430	0.180
C-D	IV	D+F+L+T_A+P	-2820	-2539	-224	-35	83	0.940	0.149	0.230
	V	1.05D+F+1.5P+ T_A	-1970	-2058	-94	28	128	0.457	0.022	0.220
	VI	1.05D+F+1.25P+ T_A+1.25E	-2444	-2183	-145	25	171	0.543	0.034	0.280
	VII	D+F+P+ T_A+E'	-2848	-2564	-226	-39	125	0.633	0.053	0.210
	II	D+F+L+1.15P	-357	-709	-293	-235	15	0.236	0.195	0.040
	III	D+F+L+T_O+E	-232	-1409	-471	-293	15	0.469	0.314	0.040
E-F	IV	D+F+L+ T_A+P	-346	-2984	-269	-133	7	0.995	0.179	0.020
	V	1.05D+F+1.5P+ T_A	-451	-2626	-197	42	23	0.584	0.046	0.040
	VI	1.05D+F+1.25P+ T_A+1.25E	-374	-2843	-231	-25	20	0.632	0.054	0.033
	VII	D+F+P+ T_A+E'	-349	-3014	-272	-135	11	0.670	0.064	0.018

TABLE 5-1

STRESS ANALYSIS RESULTS[8]

CONTAINMENT STRUCTURE - SUMMARY OF CONCRETE AND REINFORCING STEEL STRESSES (psi)

			REINFORCING STEEL			
			COMPUTED		COMPUTED VS. ALLOWABLE	
SECTION		LOAD CASE	σ_m	σ_h	$\frac{\sigma_m}{f_s}$	$\frac{\sigma_h}{f_s}$
	II	D+F+L+1.15P	-269	-16	0.009	0.001
	III	D+F+L+T_O+E	2098	694	0.070	0.023
A-B	IV	D+F+L+T_A+P	+3590	4253	0.120	0.142
	V	1.05D+F+1.5P+T_A	4760	4512	0.088	0.084
	VI	1.05D+F+1.25P+T_A+1.25E	14440	28664	0.267	0.531
	VII	D+F+P+T_A+E'	9888	16483	0.183	0.305
	II	D+F+L+1.15P	1750	4786	0.058	0.160
	III	D+F+L+T_O+E	6282	10485	0.209	0.349
C-D	IV	D+F+L+T_A+P	4040	15967	0.134	0.532
	V	1.05D+F+1.5P+T_A	147	19229	0.003	0.356
	VI	1.05D+F+1.25P+T_A+1.25E	1475	18794	0.027	0.348
	VII	D+F+P+T_A+E'	4084	16127	0.076	0.298
	II	D+F+L+1.15P	124	2148	0.004	0.072
	III	D+F+L+T_O+E	-276	5701	0.01	0.190
E-F	IV	D+F+L+T_A+P	1110	8667	0.037	0.289
	V	1.05D+F+1.5P+T_A	4080	10259	0.076	0.190
	VI	1.05D+F+1.25P+T_A+1.25E	2343	10036	0.0434	0.186
	VII	D+F+P+T_A+E'	1121	8754	0.021	0.162

TABLE 5-1

STRESS ANALYSIS RESULTS[8]

CONTAINMENT STRUCTURE - SUMMARY OF CONCRETE AND REINFORCING STEEL STRESSES (psi)

SECTION		LOAD CASE	CONCRETE COMPUTED σ_{em}	σ_{eh}	σ_{am}	σ_{ah}	τ	COMPUTED VS. ALLOWABLE $\frac{\sigma_e}{f_{ce}}$	$\frac{\sigma_a}{f_a}$	$\frac{\tau}{v}$
	II	D+F+L+1.15P	-69	-746	-154	-224	-13	0.249	0.149	0.037
	III	D+F+L+T_O+E	-1415	-1770	-683	-793	61	0.590	0.529	0.170
G-H	IV	D+F+L+T_A+P	-101	-2827	-68	-195	-11	0.942	0.130	0.310
	V	1.05D+F+1.5P+T_A	-96	-1766	114	23	-66	0.392	0.027	0.110
	VI	1.05D+F+1.25P+T_A+1.25E	-1453	-1496	-162	-221	-20	0.332	0.052	0.033
	VII	D+F+P+T_A+E'	-1529	-1683	-194	-364	1	0.374	0.086	0.002
	II	D+F+L+1.15P	-60	-653	-201	-133	1	0.218	0.134	0.003
	III	D+F+L+T_O+E	-1821	-2244	-732	-1209	-9	0.747	0.806	0.250
J-K	IV	D+F+L+T_A+P	-67	-2629	-111	-99	-2	0.876	0.074	0.006
	V	1.05D+F+1.5P+T_A	-96	-2828	169	420	2	0.628	0.099	0.003
	VI	1.05D+F+1.25P+T_A+1.25E	-1488	-957	-209	-75	5	0.331	0.049	0.008
	VII	D+F+P+T_A+E'	-1697	-1669	-311	-447	-3	0.377	0.105	0.005
	II	D+F+L+1.15P	+10	-848	-277	-718	1	0.283	0.479	0.003
	III	D+F+L+T_O+E	-621	-2012	-494	-635	-2	0.671	0.423	0.006
L-M	IV	D+F+L+T_A+P	-29	-2914	-254	-731	147	0.971	0.487	0.415
	V	1.05D+F+1.5P+T_A	-84	-2973	-263	-465	163	0.661	0.109	0.271
	VI	1.05D+F+1.25P+T_A+1.25E	-1633	-3510	-197	-914	14	0.780	0.215	0.023
	VII	D+F+P+T_A+E'	-1427	-3360	-296	-870	-6	0.745	0.205	0.010

TABLE 5-1

STRESS ANALYSIS RESULTS[8]

CONTAINMENT STRUCTURE - SUMMARY OF CONCRETE AND REINFORCING STEEL STRESSES (psi)

			REINFORCING STEEL			
			COMPUTED		COMPUTED VS. ALLOWABLE	
SECTION		LOAD CASE	σ_m	σ_h	$\frac{\sigma_m}{f_s}$	$\frac{\sigma_h}{f_s}$
	II	D+F+L+1.15P	2884	2284	0.096	0.076
	III	D+F+L+T_O+E	2616	3332	0.087	0.111
G-H	IV	D+F+L+T_A+P	16649	10293	0.555	0.343
	V	1.05D+F+1.5P+T_A	7381	15437	0.136	0.285
	VI	1.05D+F+1.25P+T_A+1.25E	23724	28024	0.440	0.520
	VII	D+F+P+T_A+E'	23595	20489	0.437	0.379
	II	D+F+L+1.15P	2368	2882	0.080	0.096
	III	D+F+L+T_O+E	5283	351	0.176	0.012
J-K	IV	D+F+L+T_A+P	11580	11410	0.386	0.380
	V	1.05D+F+1.5P+T_A	8720	10523	0.161	0.195
	VI	1.05D+F+1.25P+T_A+1.25E	29043	26964	0.537	0.499
	VII	D+F+P+T_A+E'	25474	14396	0.471	0.266
	II	D+F+L+1.15P	22007	-5482	0.734	0.183
	III	D+F+L+T_O+E	3366	1812	0.112	0.0604
L-M	IV	D+F+L+T_A+P	11216	3168	0.374	0.105
	V	1.05D+F+1.5P+T_A	13369	3063	0.247	0.057
	VI	1.05D+F+1.25P+T_A+1.25E	19995	9888	0.370	0.183
	VII	D+F+P+T_A+E'	10770	9651	0.199	0.178

TABLE 5-1

STRESS ANALYSIS RESULTS[8]

CONTAINMENT STRUCTURE - SUMMARY OF CONCRETE AND REINFORCING STEEL STRESSES (psi)

SECTION		LOAD CASE	CONCRETE COMPUTED σ_{em}	σ_{eh}	σ_{am}	σ_{ah}	τ	COMPUTED VS. ALLOWABLE $\frac{\sigma_e}{f_{ce}}$	$\frac{\sigma_a}{f_a}$	$\frac{\tau}{v}$
	II	D+F+L+1.15P	69	-362	68	76	127	0.201		0.600
	III	D+F+L+T_O+E	-911	-1204	-64	-17	48	0.669		0.220
N-O	IV	D+F+L+T_A+P	-207	-594	26	58	114	0.330	Note	0.540
	V	1.05D+F+1.5P+T_A	7	-704	20	86	149	0.196	(a)	0.413
	VI	1.05D+F+1.25P+T_A+1.25E	-861	-1203	54	52	164	0.334		0.454
	VII	D+F+P+T_A+E'	-1098	-1198	25	52	154	0.333		0.427
	II	D+F+L+1.15P	-1338	-473	56	113	74	0.743		0.350
	III	D+F+L+T_O+E	-1562	-1540	-43	-63	43	0.868		0.202
P-Q	IV	D+F+L+T_A+P	-1697	-599	-45	121	65	0.943	Note	0.306
	V	1.05D+F+1.5P+T_A	-2253	-829	-31	68	135	0.626	(a)	0.374
	VI	1.05D+F+1.25P+T_A+1.25E	-2115	-1086	-15	75	74	0.588		0.205
	VII	D+F+P+T_A+E'	-1621	-1251	-42	46	79	0.450		0.220

TABLE 5-1

STRESS ANALYSIS RESULTS[8]

CONTAINMENT STRUCTURE - SUMMARY OF CONCRETE AND REINFORCING STEEL STRESSES (psi)

			REINFORCING STEEL			
			COMPUTED		COMPUTED VS. ALLOWABLE	
SECTION		LOAD CASE	σ_m	σ_h	$\frac{\sigma_m}{f_s}$	$\frac{\sigma_h}{f_s}$
	II	D+F+L+1.15P	256	20957	0.009	0.700
	III	D+F+L+T_O+E	19168	26123	0.640	0.871
N-O	IV	D+F+L+T_A+P	13172	26362	0.440	0.878
	V	1.05D+F+1.5P+T_A	16596	35106	0.307	0.650
	VI	1.05D+F+1.25P+T_A+1.25E	30315	41218	0.561	0.763
	VII	D+F+P+T_A+E'	29196	40450	0.542	0.749
	II	D+F+L+1.15P	26933	24818	0.897	0.827
	III	D+F+L+T_O+E	24970	30500	0.832	1.000
P-Q	IV	D+F+L+T_A+P	26824	30012	0.894	1.000
	V	1.05D+F+1.5P+T_A	36983	42126	0.684	0.780
	VI	1.05D+F+1.25P+T_A+1.25E	35862	40468	0.664	0.749
	VII	D+F+P+T_A+E'	29984	41033	0.555	0.759

NOTE [a]: $f_a = 0.3 f_c'$ not applicable to base slab.

TABLE 5-1

STRESS ANALYSIS RESULTS[8]

CONTAINMENT STRUCTURE - SUMMARY OF CONCRETE AND REINFORCING STEEL STRESSES (psi)

		CONCRETE			REINFORCING STEEL	
SECTION	**LOAD CASE**	σ_{em}	σ_{eh}	τ	σ_m	σ_h
A-B	$D + F + L + T_o$	-1860	-1845	-18	-190	111
	$D + F + L + T_o + E$	-2141	-2363	20	2098	694
	$D + F + L + T_s$	-1400	-1374	-23	-4470	-4419
	$D + F + L + T_s + E$	-1466	-1526	-10	-10516	-10246
	$1.05D + F + L + 1.25P + T_A$	-653	-465	23	3700	4198
	$1.05D + F + L + 1.25P + T_A + 1.25E$	-2048	-2205	24	11731	25506
	$D + F + L + P + T_A$	-897	-794	7	3590	4253
	$D + F + L + P + T_A + E'$	-2247	-2393	17	9889	16483
C-D	$D + F + L + T_o$	7	1	43	-12,200	-6074
	$D + E + L + T_o + E$	-2281	-1393	65	8139	7912
	$D + F + L + T_s$	137	220	32	-7880	-1838
	$D + F + L + T_s + E$	-2283	-1392	-4	8101	7903
	$1.05D + F + L + 1.25P + T_A$	7	1	114	-4040	7353
	$1.05D + F + L + 1.25P + T_A + 1.25E$	-2006	-946	171	14042	10321
	$D + F + L + P + T_A$	8	1	83	-4340	-1033
	$D + F + L + P + T_A + E'$	-1545	-1209	125	9390	13818
E-F	$D + L + F + T_o$	-242	-1266	10	-1396	5701
	$D + L + F + T_o + E$	-836	-1542	15	-728	10234
	$D + F + L + T_s$	-225	-681	15	-993	1337
	$D + F + L + T_s + E$	-732	-723	30	-1135	901
	$1.05D + F + L + 1.25P + T_A$	321	-653	13	-1052	7427
	$1.05D + F + L + 1.25P + T_A + 1.25E$	-193	-2132	20	-750	52514
	$D + F + L + P + T_A$	262	-711	7	-809	9653
	$D + F + L + P + T_A + E'$	-336	-2012	11	-1691	49431

TABLE 5-1

STRESS ANALYSIS RESULTS[8]

CONTAINMENT STRUCTURE - SUMMARY OF CONCRETE AND REINFORCING STEEL STRESSES (psi)

		CONCRETE			REINFORCING STEEL	
SECTION	**LOAD CASE**	σ_{em}	σ_{eh}	τ	σ_m	σ_h
G-H	$D + F + L + T_o$	-1321	-1522	41	2622	3475
	$D + F + L + T_o + E$	-1415	-1770	61	2616	3332
	$D + F + L + T_s$	-816	-1022	-40	-1187	-1466
	$D + F + L + T_s + E$	-783	-1095	18	4114	4984
	$1.05D + F + L + 1.25P + T_A$	-2584	-2440	-32	14927	12730
	$1.05D + F + L + 1.25P + T_A + 1.25E$	-1452	-1495	-20	23724	28024
	$D + F + L + P + T_A$	-2660	-2712	-11	14972	-10960
	$D + F + L + P + T_A + E'$	-1529	-1682	1	23595	20489
J-K	$D + F + L + T_o$	-1595	-2115	-6	4228	476
	$D + E + L + T_o + E$	-1821	-2244	-9	5283	351
	$D + F + L + T_s$	-927	-1407	-8	-511	-3931
	$D + F + L + T_s + E$	-990	-1453	29	3960	-8747
	$1.05D + F + L + 1.25P + T_A$	-1029	-1648	57	-511	17727
	$1.05D + F + L + 1.25P + T_A + 1.25E$	-989	-957	5	3960	26965
	$D + L + F + T_A$	-2655	-2628	-2	11580	11410
	$D + L + F + T_A + E'$	-1696	-1669	-3	25473	14396
L-M	$D + F + L + T_o$	-304	392	-15	-2422	3821
	$D + F + L + T_o + E$	-621	-2012	-2	3366	1812
	$D + F + L + T_s$	-1039	-614	6	961	-3751
	$D + F + L + T_s + E$	-1117	-788	-16	833	-10188
	$1.05D + F + L + 1.25P + T_A$	-2005	-2980	165	37136	2914
	$1.05D + F + L + 1.25P + T_A + 1.25E$	-1633	-3510	14	19995	9888
	$D + F + L + P + T_A$	-1845	-2914	147	28111	3168
	$D + F + L + P + T_A + E'$	-1427	-3360	-6	10770	9651

TABLE 5-1

STRESS ANALYSIS RESULTS[8]

CONTAINMENT STRUCTURE - SUMMARY OF CONCRETE AND REINFORCING STEEL STRESSES (psi)

		CONCRETE			REINFORCING STEEL	
SECTION	**LOAD CASE**	σ_{em}	σ_{eh}	τ	σ_m	σ_h
N-O	$D + F + L + T_o$	-708	-696	24	12251	15290
	$D + F + L + T_o + E$	-910	-1070	48	19168	26123
	$D + F + L + T_s$	-537	-492	32	8742	5101
	$D + F + L + T_s + E$	-930	-1080	33	20719	27297
	$1.05D + F + L + 1.25P + T_A$	-484	-728	98	22724	30046
	$1.05D + F + L + 1.25P + T_A + 1.25E$	-861	-1203	164	30315	41218
	$D + F + L + P + T_A$	-763	-743	114	25316	28528
	$D + F + L + P + T_A + E'$	-1098	-1198	154	29196	40450
P-Q	$D + F + L + T_o$	-1251	-688	22	17161	15582
	$D + F + L + T_o + E$	-1562	1355	43	24970	30500
	$D + F + L + T_s$	-911	-446	44	8506	3814
	$D + F + L + T_s + E$	-1165	-630	60	17945	13720
	$1.05D + F + L + 1.25P + T_A$	-1821	-670	44	32542	30141
	$1.05D + F + L + 1.25P + T_A + 1.25E$	-2115	-1086	74	35862	40468
	$D + F + L + P + T_A$	-1697	-599	65	26824	30012
	$D + F + L + P + T_A + E'$	-1621	-1251	79	29984	41033

TABLE 5-1

STRESS ANALYSIS RESULTS[8]

NOTES:

1. Loading Cases I, II, III, & IV are working stress analysis whereas Loading Cases V, VI, & VII are yield stress analysis.
2. For notation see next page.
3. All concrete extreme fiber stresses sc are for the inside surface. Outside surfaces stresses are indicated by ( ). The stresses listed are the controlling stresses for that section.
4. Computed vs. allowable ratios for Cases V, VI, and VII include appropriate ϕ factors, e.g.,f $\sigma_a/f_a = \sigma_a/\phi_a(f_c)$.
5. Allowable shear stresses include stirrups whenever applicable.
6. Deviations in allowable stresses are in accordance with Section 5.1.2.2.
7. Reinforcing steel is Type A615, GR 60.
8. See Appendix 5E for later tables associated with an evaluation to reduce the original amount of required containment prestress.

NOTATION

D	Dead load
F	Prestress
P	LOCA pressure load
E	Earthquake (OBE)
E'	Earthquake (SSE)
T_A	Accident temperature
f_c	Concrete compressive strength at age of 28 days
f_y	Steel re-bar yield stress
f_a	Allowable concrete axial stress
f_{ce}	Allowable concrete axial & flexure stress
y	Allowable concrete shear stress including stirrups if applicable
f_s	Allowable steel stress
σ_a	Nominal membrane stress
σ_e	Combined axial & flexure nominal stress
τ	Actual shear stress
h	Subscript indicating hoop direction
m	Subscript indicating meridional direction
p_h	Hoop steel percentage
p_m	Meridional steel percentage

TABLE 5-1

STRESS ANALYSIS RESULTS[8]

+	Tensile stresses
-	Compressive stresses
	Cracked section analysis
ν_{ci}	Section 5.1.2.2 (loads necessary to cause structural yielding)
ν_{cw}	Section 5.1.2.2 (loads necessary to cause structural yielding)

TABLE 5-2

ASSUMED INTERNALLY GENERATED MISSILES IN CONTAINMENT STRUCTURE

	ITEM AND LOCATION	WEIGHT	MASS/ AREA lb/in^2	SOURCE [b,c]	SHAPE	IMPACT VELOCITY ft/sec	POINT OF IMPACT
I.	REACTOR VESSEL						
	a) Closure Head Nut	116	.0034	1	Cylindrical	35.5	Overhead Shielding Slab
	b) Closure Head Nut and Stud	710	.0477	1	Cylindrical	21.2	Overhead Shielding Slab
	c) Instrument Assembly	335	.0445[a]	2	Rod	49.4	Overhead Shielding Slab
	d) Instrument	165	.0219[a]	2	Flat Rod	211	Overhead Shielding Slab
II.	STEAM GENERATOR						
	a) Primary Manway Cover	1000	6.57[a]	2	Disk	156.6	Steam Generator Walls
	b) Primary Manway Cover Stud and Nut	24	7.64	1	Rod	33	Steam Generator Walls
	c) Secondary Handhole Cover	150	3.76[a]	2	Disk	181	Steam Generator Walls
	d) Secondary Handhole Cover Stud and Nut	4	4.04	1	Rod	17.9	Steam Generator Walls
	e) Secondary Manway Stud	4.67	.0098	1	Rod	506.7	Pressurizer Shield Wall
	f) Inspection Port Cover	30	1.72	2	Disk	668	Steam Generator Walls
	g) Inspection Port Cover Stud and Nut	1.33	3.02	1	Rod	1295	Steam Generator Walls
III.	PRESSURIZER						
	a) Safety Valve & Flange	550/800	.4540	2	Cylindrical	97.2/80.6	Pressurizer Shield Wall
	b) Valve Flange Bolt	3.75	.0079	1	Rod	16.5	Pressurizer Shield Wall
	c) Relief Valve & Flange	150	.0311[a]	2	Cylindrical	150	Pressurizer Shield Wall
	d) Manway Cover	680	.0150[a]	2	Disk	369	Pressurizer Shield Wall
	e) Upper Temp. Element	2.75	.0052[a]	2	Rod	81.8	Pressurizer Shield Wall
	f) Lower Temp. Element	3	.0056[a]	2	Rod	80.2	Pressurizer Shield Wall
	g) Safety Valve	200	.1648	2	Cylindrical	158	Pressurizer Shield Wall
IV.	CONTROL ROD DRIVER	1100	.0365	2	Cylindrical	58	Overhead Missile Shield
V.	MAIN PUMP & PIPE						
	a) Temp. Nozzle & Rtd	11.1	.0209[a]	2	Cylindrical	81.3	Secondary Shield Wall
VI.	SURGE & SPRAY LINES						
	a) Thermal Well & Rtd	1.75	.0033[a]	2	Cylindrical	105	Secondary Shield Wall

TABLE 5-2

ASSUMED INTERNALLY GENERATED MISSILES IN CONTAINMENT STRUCTURE

	ITEM AND LOCATION	WEIGHT	MASS/ AREA lb/in^2	SOURCE (b,c)	SHAPE	IMPACT VELOCITY ft/sec	POINT OF IMPACT
VII.	SHUTDOWN COOLING						
	a) Line Valve Stem	85	.0450	2	Cylindrical	50.4	Secondary Shield Wall

---

[a] Cross-section used is projected edge area (dia x thk) all other areas are minimum projected area.
[b] Stored mechanical strain energy converted to kinetic energy by separation of stud.
[c] Hydrostatic pressure force converted to fluid jet force by separation of mechanical restraint.